To the Graduate Council:

I am submitting herewith a thesis written by Daniel Steven Erb entitled "The Economic Analysis of a Natural Gas Fired Magnetohydrodynamic/Steam Combined Cycle Power Plant." I have examined the final copy for form and content and recommend that it be accepted in partial fulfillment of the requirements for the degree of Master of Science, with a major in Mechanical Engineering.

Harold J. Schmidt

Harold J. Schmidt, Major Professor

We have read this thesis
and recommend its acceptance:

Lloyd W. Crawford

James N. Chapman

Accepted for the Council:

C. W. Minkel

Associate Vice Chancellor
and Dean of The Graduate School

STATEMENT OF PERMISSION TO USE

In presenting this thesis in partial fulfillment of the requirements for a Master's degree at The University of Tennessee, Knoxville, I agree that the library shall make it available to borrowers under the rules of the Library. Brief quotations from this thesis are allowable without special permission, provided that accurate acknowledgment of the source is made.

Permission for extensive quotation from or reproduction of this thesis may be granted by my major professor, or in his absence, by the Head of Interlibrary Services when, in the opinion of either, the proposed use of the material is for scholarly purposes. Any copying or use of the material in this thesis for financial gain shall not be allowed without my written permission.

Signature ____________________

Date 12/2/94

THE ECONOMIC ANALYSIS OF A NATURAL GAS FIRED MAGNETOHYDRODYNAMIC/STEAM COMBINED CYCLE POWER PLANT

A Thesis

Presented for the

Master of Science

Degree

The University of Tennessee, Knoxville

Daniel Steven Erb

December 1994

DEDICATION

This thesis is dedicated to my loving family--past, present and future--and to all the students who only need some encouragement to explore the many opportunities that a formal education affords.

ACKNOWLEDGMENTS

I would first like to thank all my committee members for the time and energy they spent on helping me prepare this thesis. Specifically I would like to thank Dr. Jim Chapman for accepting me as one of his Graduate Research Assistants, for always being available as a ready reference regarding the SYSTEMS computer code used in this thesis, and for teaching me the theory of magnetohydrodynamics. I furthermore thank Dr. Harold Schmidt for his many helpful suggestions and guidance throughout the development of this thesis.

Next I would like to thank my sister Robin and brother Robert for inspiring me, by their example, to achieve the high academic standards necessary to become a graduate research assistant. I would like to thank my brother John, sister MIchelle, and all my friends that encouraged me to persevere and also my mother, Janice, and father, Robert, for providing me with so many great experiences throughout my life and supporting me along most of the paths I chose to explore. Lastly, I would like to thank my fiancée, Diane Rios, whose love enhanced my drive to graduate and start a life in the "real" world.

ABSTRACT

Combined cycle base load power plants are an alternative concept for future commercial electricity production. Magnetohydrodynamic power generation in a combined cycle has been shown to be an efficient and cost effective process for such applications. In any large scale endeavor, it is necessary to establish the economic viability of the concept before any serious pursuit of its implementation can be considered. The economic viability for coal fired magnetohydrodynamic/steam combined cycle systems has been extensively studied and shown to be cost effective.

Natural gas as a primary fuel has several advantages over coal in magnetohydrodynamic power generation including the absence of slag forming compounds. Slag not only can have detrimental effects in combustion derived flow streams but also is an undesirable solid waste product. Natural gas is an environmentally acceptable fuel because the exhaust products are less destructive to the environment. A benefit for using natural gas in MHD operation involves the absence of any slag forming compounds.

This document describes a study of the feasibility of using natural gas as an alternate fuel for the highly efficient MHD/steam combined cycle power plant. The analysis was conducted by modifying an existing coal fired MHD/steam combined cycle computer modeling program. The results obtained, following parametric analysis for optimization, suggest that natural gas fired operation can produce electricity at a lower cost than present conventional steam generators operating on coal.

TABLE OF CONTENTS

LIST OF FIGURES

Figure **Page**

LIST OF ABBREVIATIONS

Balance of Plant . . . . .BOP

Coefficient of Performance . . . . .COP

Conceptual Design Study of a Potential Early Commercial MHD Power Plant . . . . CSPEC

Cost of Electricity . . . . COE

Diagonal Conducting Wall . . . . DCW

Electrostatic Precipitator . . . . ESP

Energy Conversion Alternatives Study . . . . ECAS

Federal Energy Regulatory Commission . . . . FERC

Gross National Product . . . . GNP

High Temperature Air Heater . . . . HTAH

Intermediate Temperature Air Heater . . . . ITAH

Lower Heating Value . . . . LHV

Magnetohydrodynamic . . . . MHD

Organization of Petroleum Exporting Countries . . . . OPEC

Parametric Study of Potential Early Commercial MHD Power Plants . . . PSPEC

LIST OF SYMBOLS

$\mathbf{B}$, B .... Magnetic Field Vector, Scalar

CH_4 .... Methane

CO_2 .... Carbon Dioxide

d .... Hydraulic Diameter

Δ .... Lumped Boundary Layer Dimensionless Voltage Drop

$\mathbf{E}$ .... Electric Field Vector

E_x .... Hall Electric Field Component

E_y .... Faraday Electric Field Component

h .... Static Enthalpy

J_x .... Hall Current Density Component

J_y .... Faraday Current Density Component

K_2CO_3 .... Potassium Carbonate

K_2SO_4 .... Potassium Sulfate

NO_X .... Nitrogen Oxides

p .... Static Pressure

$\dot{q}_w$ .... Wall Heat Loss Term

ρ .... Plasma Density

σ .... Scalar Conductivity

T_L .... Low Temperature Reservoir

T_H .... High Temperature Reservoir

τ_w .... Wall Shear Stress

$\mathbf{u}$, u .... Plasma Velocity Vector, Scalar

$\mathbf{u^*}$ .... Electron Drift Velocity Vector

V_d .... Lumped Voltage Loss Term

V_T .... Terminal Voltage

CHAPTER I

INTRODUCTION

Magnetohydrodynamics is the study of electrically conducting fluid flow in the presence of a magnetic field. This relatively unexploited method of electrical energy production has the potential for both cost effective and thermally efficient power generation. Power generating ability can be linked to the success of every industrialized nation. While early technology was geared towards producing cheap electrical energy by any means available, today's political climate demands a more comprehensive world view outlook. Present day objectives include reducing natural resource consumption and limiting many environmental impacts. To this end, the high technology method of power generation named magnetohydrodynamics (MHD) is suggested as a means for meeting these objectives. While the renewable energy sources may be the hope for the future, present technological studies suggest that the high efficiency, and environmentally friendly MHD plant is cost effective today. Coal fired MHD plants studied in the past were considered environmentally friendly for two reasons, first the operation assured virtual elimination of sulfur and nitrogen oxides, the acid rain precursors, from the exhaust stream and second high efficiency plants require less energy input per energy output which reduces both the consumption of resources and the production of pollution. Thus the high efficiency and environmentally friendly MHD concept appears to go hand in hand with today's political climate.

Electrical energy provides instant power at the touch of a button. This particular energy source has been a part of American life for so long it is rarely given notice except when monthly utility bills arrive. The existence of electrical outlets in almost every structure built in America, justifies this peace of mind and freedom that Americans enjoy regarding their unrestricted access to energy. The ease of access, for this incredibly flexible resource, is one reason for the ever increasing number of consumer products and demands. Electrically powered products are presently in competition with products originally powered by more convenient combustion methods, such as lawn mowers, compressors, stoves, and water heaters. Electric power is even on the way to becoming the fuel for the zero emission automobiles of tomorrow. This drive towards an electric powered society is also, in part, due to the desire to localize pollution. For example, even though Los Angeles air pollution levels have been on the decline for the last several years, due to stricter emission regulations, the city is still pursuing a zero emission vehicle. The use of electric power for personal vehicles clearly won't reduce fuel consumption, but the ability to relocate the pollution away from the city is apparently worth the extra costs that will be incurred by building more electric power plants, development of a city wide electric charging infrastructure, and battery disposal.

Electrical energy is far from being a power source available to all of the world's inhabitants. General energy consumption, it has been suggested, is linearly related to a country's gross national product (GNP) (Krenz, 1976). This uneven distribution is the reason behind the necessary energy importation practices of the more industrialized countries. In 1973, the Organization of Petroleum Exporting Countries (OPEC) staged an oil embargo which clearly demonstrated the pitfalls of dependency on foreign energy reserves. Even with this knowledge, the practice of gluttonous energy importation continues today. While the present political climate favors more efficient energy production, the reality of maintaining a high GNP must support the use of cheaper fuels and less efficient energy production methods.

Following 1973, the topics of limited world energy resources and the imbalances of resource consumption surfaced. In 1980, an international energy symposium was held in Knoxville, Tennessee entitled *World Energy Production and Productivity*. The topics for discussion included defining "the nature of the problem" and "the role of technology", as well as, discussing the "critical paths, conflicts, and constraints" towards an efficient energy future. Although the different speaker's predictions for the future varied considerably, a general consensus existed as to the severity of the increasing energy trends. Discussions regarding local versus central power generation, and the need for subsidized "efficient building" improvements also were discussed. In general, the dialog most often spoke of the political realities of energy control and the supremacy available to countries pursuing increased utilization.

After the oil embargo of the 70's, the United States promoted any energy research focused toward utilization of its abundant coal reserves. The target goals were both increased efficiency and reduced pollution for the coal burning power plants. Inefficient operation results in the emission of unnecessary amounts of global warming carbon dioxide (CO_2), sulfur oxides, nitrogen oxides, and thermal pollution. Thermal pollution is a term for waste heat that the environment must absorb either in the atmosphere or in watershed streams. As far as the air pollution components are concerned, sulfur oxide emissions were by far the most harmful coal combustion byproducts. When the sulfur oxides reacted with moisture in the clouds, sulfuric acid was produced which damaged the environment in the form of acid rain. The nitrogen oxides, or NO_x, can also contribute to acid rain but it is better known as a producer of the unhealthy brown haze ("smog") seen in the larger cities.

Although improvements were made, and coal still represents a sizable percentage of fuels combusted for the generation of electricity, U. S. policy has moved away from this resource. Present U. S. funding endorses the more environmentally friendly natural gas resource for power generation. According to 1990 statistics, the U. S. is responsible for producing a large fraction (25%), of the world's natural gas supply. The Department of Energy in November of 1992, announced a $600 million research and development program directed at developing a natural gas fueled turbine based combined cycle power plant with 60% overall efficiency based on the gas Lower Heating Value (LHV) of 21518 Btu/lb.

A Carnot engine offers the highest thermal efficiency possible for a cycle operating between fixed temperature reservoirs. The thermal efficiency equation when using an ideal gas as the working fluid is,

$$\% \text{ efficiency} = (1 - T_L/T_H) \times 100 \qquad (1)$$

with T_L and T_H representing the low and high reservoir temperatures, respectively. Since the low temperature is fixed by terrestrial atmosphere or water temperatures which comprise the thermal sink, the only practical method to achieve a higher efficiency is by raising the input temperature of the cycle. Because MHD electrical generators require no mechanical moving parts, the inlet temperatures to the MHD can be as high as material limits will allow. On the other hand, in a gas turbine, for example, mechanical and thermal stresses severely limit sustainable temperatures. To reach the same inlet temperature as an MHD generator, blade cooling and new high strength blade composites would be required. Therefore, barring some revolutionary concept, at present there is no foreseeable way for the turbine inlet temperature to exceed the inlet temperatures available with a MHD generator.

Consequently, the need for exploring natural gas fired MHD/steam combined cycle power plants can be indirectly tied to all of the preceding discussion. While considerable amounts of money are spent researching energy distributions and the need for the U. S. to curb its insatiable thirst for resources, the facts show that world electricity consumption is on the rise across the board. Many operating power plants, in the United States are old, and new plants will be required to keep up with presently increasing demand trends. At the same time, third world countries are now reaching the industrial age and demanding more power generating capabilities. Greater numbers and more efficient base load power plants are a real necessity to meet future electricity demands.

Open cycle magnetohydrodynamic/steam central power, using coal as the fuel, was determined to be the most economically viable option for research in the late 1970's. This finding was partially based on the earlier discussed environmentally friendly attributes which MHD systems inherently possess when burning coal. While MHD technology bloomed during the heavily funded research years of the early 80's, the inability to overcome slag polarization, expensive seed regeneration, and poor generator and material durability, resulted in significantly reduced research support in the 90's. With the policy trends now aimed towards using natural gas, it is logical to again look toward the high efficiency MHD/steam combined cycle power plant while realizing that the first two slag associated problems cited above would be either reduced or eliminated if natural gas is the fuel.

Recognizing that the use of natural gas is being encouraged, a significant disadvantage to funding the development of the advanced MHD/steam combined cycle power plant lies with the high temperature chemistry of natural gas combustion products since natural gas has a lower carbon to hydrogen ratio than coal. Natural gas is predominantly comprised of methane (CH_4), as much as 94%, which when burned produces a larger percent of water products than the earlier researched coal. At the high temperatures required for the MHD process, the water molecule can dissociate forming OH radicals. The problem with OH radicals involves their electrophilic characteristics and large collision cross sections. Because free electrons become attached to the OH radical, these electrons can no longer contribute to the conductivity process in the regime of central station power MHD.

The need for an economical solution to present energy demands is the driving factor behind this thesis topic. Regardless of high efficiency and pollution reduction characteristics, any underdeveloped power plant technology must have clear cost benefits associated with its utilization to receive research funding. The first step towards this aim, following the ECAS study methodology, is to perform a parametric analysis based on an appropriate model. For this study an existing coal-fired MHD economic analysis model was modified to allow the evaluation of natural gas as a suitable fuel. The modifications included modifying the seed recovery process, removing all coal handling processes, changing the input chemistry, omitting slag losses, and making the respective adjustments to the economic calculations.

The following chapters are organized to develop an understanding of the MHD process and present material which illustrates the validity of the concept. Specifically, in Chapter II, the history, theory, and comparison of natural gas with coal, as fuels for magnetohydrodynamics, are presented and discussed. Chapter III provides a detailed discussion of the computational program development and the subroutine interactions which were used to evaluate the modelled MHD/steam combined cycle system. The parametric results, generated by the code discussed in Chapter III, are presented in Chapter IV followed by the summary and conclusions in Chapter V.

CHAPTER II

MAGNETOHYDRODYNAMICS

The History of MHD

The basic theory behind magnetohydrodynamics (MHD) has been available since 1831, with Faraday's discovery of electromagnetic induction. Faraday found that electricity could be generated by passing an electrical conductor, solid or fluid, through a magnetic field. Around 1910, inventors began to receive patents for different flowing fluid power generating schemes that were based on Faraday's earlier work. While the inventors tried to harness the fluid's energy, promised by the simple laws of magnetic induction, it wasn't until 1959 that an experimental MHD generator was designed and built that produced any theory verifying results. The Avco Mark I, 10 kW, experimental generator design was conceived and built only after considerable advances in the field of plasma physics were achieved. Further discoveries in plasma physics are still sought today, 35 years later, which will eventually enable MHD power plants to efficiently utilize the world's limited natural resources.

The results obtained in the Avco Mark I test prompted great interest and excitement in the MHD field. To further the theory and promote MHD power generation, annual symposia, both domestic and international, began convening as early as 1960 and 1962 respectively. Although at first many different countries were involved in the early development stages of MHD, only a handful of countries continually funded this particular avenue. Namely, while China, England, France, Germany, India, Italy, Japan, Poland, Russia, and the U. S. were initially interested in the technology, only China, Japan, Russia, and the U. S. still explore the concept through government funding. Fortunately

Australia, Israel, and the Netherlands are also beginning research aimed at unlocking the great potential that MHD promises for the future.

During the U. S. funded research efforts of the mid 1970's, discussed in the introduction, many studies were aimed at coal based alternative energy production. One of the most significant studies for MHD development was entitled the Energy Conversion Alternatives Study (ECAS) (Seikel and Harris, 1976). The ECAS study included parametric analyses, conceptual designs, and implementation assessments. The parametric analyses were performed on ten power plant options, while both the conceptual designs and the implementation assessments were conducted on eleven power plant models. The various models considered included; open and closed cycle MHD, open and closed turbine systems, and fuel cells. The inclusion of the different MHD systems in the ECAS study most assuredly could be linked to the corresponding development of superconducting magnets during the same time period. The ECAS summary report concluded that the open-cycle coal-fired recuperatively-preheated MHD system concept had the greatest potential to produce a low Cost of Electricity (COE).

One easily recognizable advantage supporting the MHD electricity generating concept, involved the reduced number of required energy conversion steps. The MHD process converts thermal energy directly into electrical energy; whereas, conventional turbine driven generators convert thermal energy into both kinetic and mechanical forms prior to producing electrical energy. While MHD generators have been conceived with various radial, vortical, or linear duct geometries--in the base load power plant studies--only the linear duct geometry has been considered because of the simple geometry, inherent durability, and ease of implementation and maintenance.

As a consequence of the ECAS report, many additional studies were sponsored through the 1980's. The Parametric Study of Potential Early Commercial MHD power plants (PSPEC) (Hals, 1981), which concluded in September 1981, and the Conceptual Design Study of a Potential Early Commercial MHD power plants (CSPEC) (Staiger and Penko,1982), which concluded in January 1982, both corroborated the potential low COE benefits that MHD base load power plants could provide. Considerable funds continued to support the development of the MHD combined cycle plant until the early part of 1993. The inability to find immediate solutions to: 1) the polarization effects in the MHD channel, 2) the incurred expense associated with seed regeneration, 3) poor channel durability, and 4) the lack of utility interest, resulted in the reduction of government funding.

The Basic Theory of MHD

An induced electric field exists whenever an electrical conductor is moved transverse to a magnetic field. If a conductor is moved with velocity u through a magnetic field B, an electric field E will be induced in a direction that is mutually orthogonal to both u and B. The magnitude of E is dependent on the angle existing between the conductor motion and the magnetic field directions. This relationship may be expressed mathematically using the following vector equation,

$$\mathbf{E} = \mathbf{u} \times \mathbf{B} \qquad (2)$$

For MHD applications of interest, the magnetic field would be applied by a superconducting magnet and the moving conductor would be a steady flow of high temperature plasma. The relations are shown in figure 1 for a linear duct geometry. Using the coordinate system shown, the plasma velocity **u** is

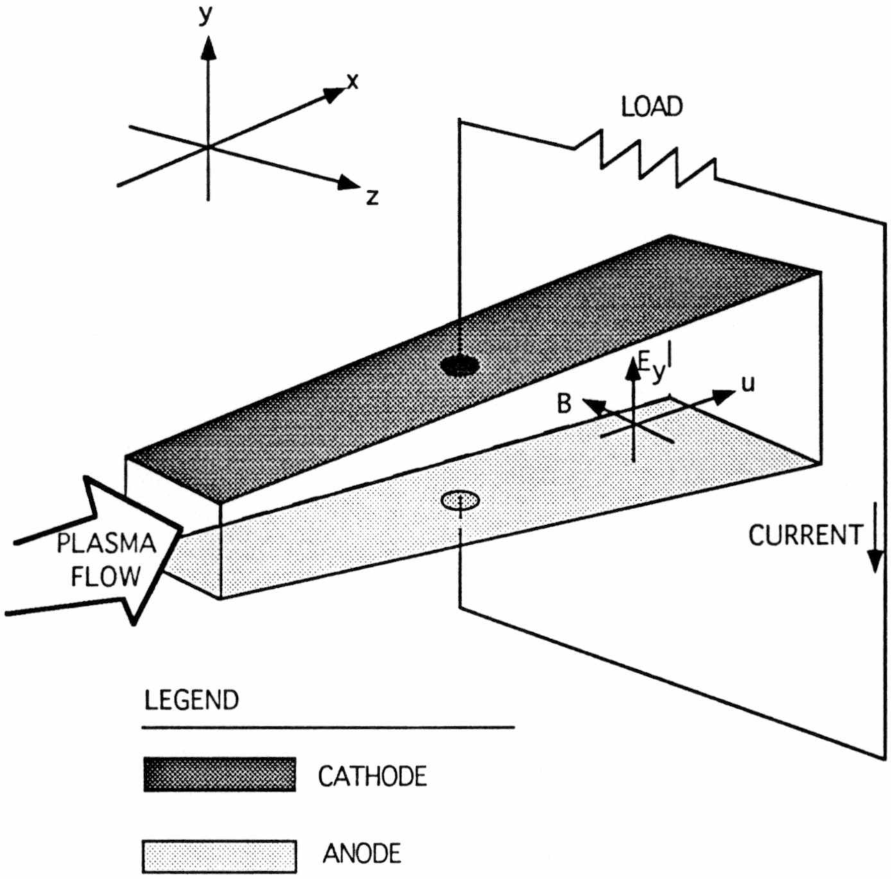

Figure 1. Linear Duct MHD Generator

directed along the x-axis, the applied magnetic field **B** is taken to be along the negative z-axis, and the resulting induced electric field **E** is along the y-axis.

The flow, or high temperature plasma, is obtained by expanding a seeded combustion gas through a nozzle. Seeding a gas, in terms of a MHD application, is the process of adding an easily ionized alkali metal salt to the combustion process. The introduction of an alkali metal such as potassium or cesium is required to ensure that a conductive plasma may enter the MHD channel at the static temperature following the nozzle expansion. By observation, the flowing plasma velocity, **u** in equation 2, needs to be perpendicular to the applied magnetic field **B** to maximize **E**. The mutually orthogonal induced electric field is in the positive y-direction and is designated E_y, as shown in figure 1. The y-direction field and current are conventionally termed the Faraday field and Faraday current, respectively.

In a duct constructed of non-conducting ceramic materials, the free electrons and positive ion counterparts would tend to separate along the y-axis until a steady state attractive force was developed between them. By replacing the insulator walls sloped in the x-z planes with electrodes, and connecting the electrodes through an electrical load, a current path forms and power may be extracted. The resulting Faraday current, given the designation J_y, consists of electrons drifting relative to the plasma flow in the y-direction which can be represented by **u'**. Applying equation 2 to this relative motion, which is orthogonal to the applied magnetic field, results in an induced electric field directed in the negative x-direction. If a current path forms in the x-direction as well, the resulting flow would be labeled J_x. The x-direction electric field (Ex) and current (Jx) are conventionally termed the Hall field and Hall current, respectively.

The developing Hall field was originally considered a negative consequence of using a conducting plasma as the working fluid in a MHD generator design. Further experimentation with conducting plasmas revealed that the Hall field could actually achieve the same magnitude as the Faraday field. The realization made apparent the fact that the induced electric field always tends to be 2-dimensional and is an important consideration for MHD design technology. The MHD channel could now be configured to minimize any one of the four basic operating components; namely, the Hall current, the Hall field, the Faraday current, or the Faraday field. Each configuration has inherent positive and negative aspects associated with its physical application. The four generator designs types, shown in figure 2, are the continuous and segmented Faraday, the Hall type, and the Diagonally Conducting Wall (DCW).

The continuous electrode Faraday generator consists of two electrodes placed across the channel perpendicular to the transverse current flow (J_y). The other two sides are again insulator walls. In this configuration the length wise electric field, or Hall field E_x, is zero since it is essentially shorted by the continuous electrode, but an axial Hall current, J_x, still exists and this current is allowed to circulate by way of the electrode surfaces rather than through the load and thus represents a loss which only serves to heat the plasma. To combat the ill effects of the Hall current, the electrode can be segmented by placing insulator sections between electrode sections. This is the basis for the segmented Faraday design shown in figure 2. The disadvantage of the segmented Faraday design is that once the electrode has been segmented and the shorting path for the Hall current eliminated, the Hall current becomes zero but the Hall field E_x develops a differing potential on each of the segmented electrodes. Loading the segmented Faraday design is very complex since each pair of the segmented electrodes requires its own load. Of all the MHD

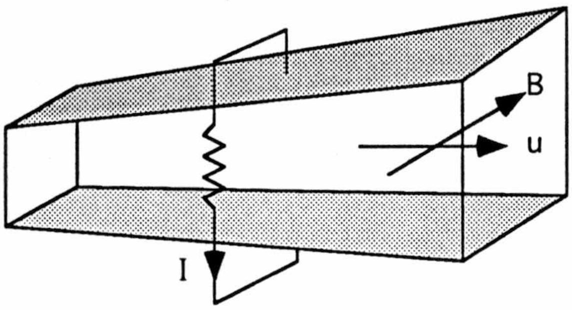

(a) Continuous Electrode, $E_x = 0$

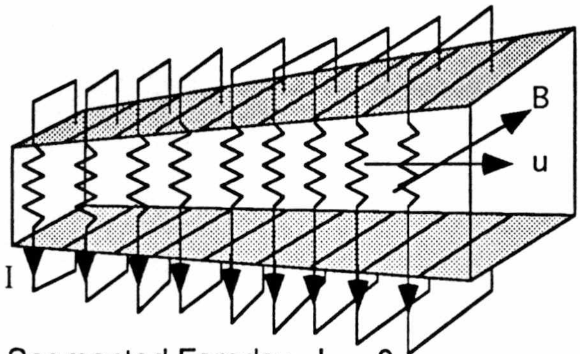

(b) Segmented Faraday, $J_x = 0$

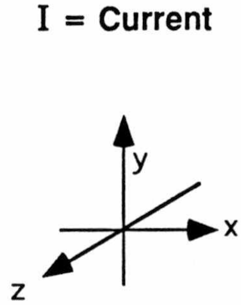

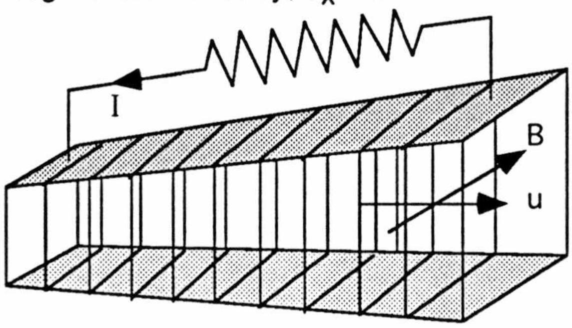

(c) Hall Type, $E_y = 0$

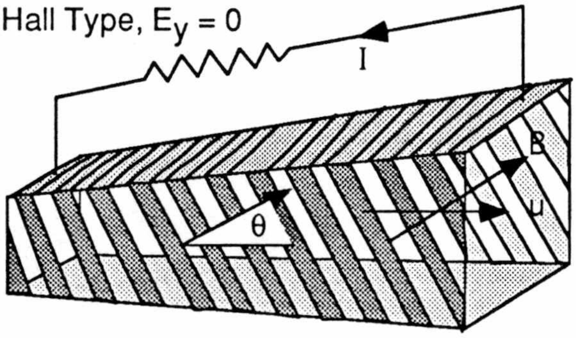

(d) Diagonal Conducting Wall (DCW), $\tan \theta = E_y/E_x$

Figure 2. Linear MHD Generator Configurations

generator channels, the segmented Faraday configuration theoretically produces the greatest amount of power.

Another way of developing power is to maximize the Hall current. By effectively shorting each of the segmented electrode pairs along the axial direction, while again having each electrode separated by insulation sections, the transverse Faraday electric field E_y can be eliminated. When the load is placed between the first and last electrode pairs along the axial direction, power can be developed by the resulting axial Hall current, J_x, and Hall electric field E_x. Since a developed Hall current has a smaller amplitude than a representative Faraday current, the theoretical amount of Hall power available can only approach that of the Faraday design when heavily loaded. Once it was proven that this method of power production was indeed possible, the idea of using frame electrode segments was explored. Use of electrode frames both ensures the elimination of the Faraday current and simplifies the fabrication of the alternating conductor-insulator frame generator.

The last configuration to discuss is the DCW generator. Conceptually, electrodes on the top of a segmented Faraday generator can be shorted with same potential electrodes on the bottom. As with the Hall generator, the shorting conduit could be composed of a continuous electrode. This design would use conducting frames positioned at a wall angle determined by performance requirements. Defining θ as the angle between the plasma flow and an angle perpendicular to the wall electrode, the relationship $\tan \theta = E_y/E_x$ can be derived (Wu, 1976). By selecting the angle that eliminates the Hall current the DCW design can operate conceptually as if it were a Faraday generator. The benefit of using diagonally conducting walls in a Faraday mode involves the ability to load the generator over multiple electrodes as if in a two terminal mode of operation similar to that of both the Hall and continuous electrode. Thus the DCW provides a functional compromise between the theoretical performance possible from the Faraday and Hall generator designs. In the two limiting cases of $\theta = 0$ and $\theta = 90$ degrees, the DCW design actually reduces to the Hall and Faraday modes of operation respectively. The wall angle θ can be optimized only over limited sections of channel. The continually changing channel conditions.limit the optimization and consequently the overall performance capability of this configuration. The greatest benefit of the DCW design involves the ability to operate the channel with performance approaching a segmented Faraday channel without the need for the great number of individually loaded sections.

During early duct geometry experiments, the four electrode configuration options were evaluated. The continuous Faraday and Hall design types, while having benefits of operational simplicity, have been evaluated in literature as producing poor experimental results. The segmented Faraday design, while offering the best channel performance, required very complex wiring schemes to fully develop the energy. Therefore the DCW generator was determined to be the best duct configuration of the four types for central power generation. For optimum performance, the DCW generator must function in a Faraday mode of operation. Since, as stated above, the conditions are ever changing in the generator, the ability to fully restrict the development of axial current along the whole channel length with a constant wall angle is not practical and can only be approximated in practice. For design purposes, a segmented Faraday operation can be explored as an early approximation of how the DCW might be able to perform. Based on current and field data obtained along a segmented Faraday channel, the best wall angle design choice for a DCW generator can be approximated. The wall angle is selected to eliminate the Hall current and allow the generator to operate essentially in the segmented Faraday mode.

This paper explores the performance of a segmented Faraday channel only; final determination of a practical wall angle for DCW operation is beyond the scope of this paper.

The complete governing equations for a MHD generator are far more complex than the equation expressed above. Use of the fluidic conservation equations for mass, momentum, and energy, Ohm's law, and the Maxwell relationships are required to properly model the physical interaction occurring in the generator channel. Under the simplifying assumption of a one dimensional steady state flow, the complex relationships mentioned above reduce to mathematically tractable equations evaluated by specifying different performance criterion. A more detailed explanation of the MHD theory is available in the cited works of R. J. Rosa and G. J. Womack (Rosa, 1968 and Womack, 1969). The reduced equations used to evaluate the model MHD generator are listed explicitly in Chapter III under the subsection title CHAN - The MHD Performance Subroutine.

MHD Performance With Natural Gas versus Coal

For the previous studies of MHD using coal as an energy source, it was noted that slag polarization effects (electrical shorting), seed regeneration, and durability were primary concerns that had not been fully overcome. The idea of using natural gas as the energy source, while far from revolutionary (Russia has been studying this avenue for years), presently requires investigation based on its apparent elimination of the first two concerns listed above. Slag is a glassy substance that forms from the impurities found in coal and is comprised of metallic oxides and ceramics. When coal is the fuel source used, the slag and entrained seed compounds condense on the cooled walls of the channel and form a thermally insulating layer between the electrodes and the conducting ionized gas. While the slag thermal insulation layer provides benefits of shielding of the electrodes from the high temperature gas, the resulting polarization is detrimental to the channel performance. Molten slag is also a solvent of other ceramic materials and as such, high temperature ceramics are eroded in a molten slag environment. With the use of natural gas, the thickness of this interfering layer could be reduced if not eliminated and high temperature ceramic electrical insulators could be effectively used. Conversely, similar effects may result if condensed seed compounds form a film over consecutive electrodes or penetrate the insulator sections. Clearly further experimental data is required on this subject.

The seed recovery would be greatly improved and simplified with the use of natural gas over coal. When coal is used as the fuel the seed reacts with the sulfur impurities within the coal, and becomes entrained in the flowing slag layer. The resulting potassium compounds, primarily K_2SO_4, require chemical processing to recover the potassium and then further processing to reform the potassium carbonate, K_2CO_3, seeding compound with hydrogen sulfide, H_2S, as a generated waste product. With the use of natural gas as the fuel, the seeding compound is expected to reform upon reaching the lower temperatures downstream of the MHD channel. Minimal processing would be required for the recovery of seeding compound but rather an appropriate particulate collection method such as an electrostatic precipitator (ESP) or baghouse would be required. Even the final performance concern, the channel reliability problems, may be directly linked to slag layer interference and hence improved with the use of natural gas.

CHAPTER III

THE SYSTEMS CODE

Background History of the Code

In 1976, different concepts regarding coal fired advanced power plant design were compared in a report referred to as the Energy Conversion Alternatives Study or ECAS. The initial report included three different types of magnetohydrodynamic (MHD) combined cycle plants among the ten systems studied; specifically, they were open and closed cycle plasma based and liquid metal MHD topping cycle plants. The results of the interagency funded study showed that "open-cycle, coal-fired, recuperatively-preheated MHD systems have potentially one of the highest coal-pile-to-bus-bar efficiencies" and also "one of the lowest cost of electricity systems studied" (Seikel and Harris, 1976). Following the ECAS report, extensive energy and resources were directed at developing the necessary technology to exploit this potential.

In 1977, in response to the above referenced activity, a computer model for predicting the cost and performance of MHD combined cycle coal fired systems was developed at the University of Tennessee Space Institute (UTSI). The computer model, termed Chapman I, was written in FORTRAN code and consisted of a main routine and four major subroutines; SINGH, BECKER, DESIGN 3, and NASA SP-273 (Chapman, et al. 1985). The first two subroutines were named after students attending an advanced combustion course. SINGH is a plant systems' performance program, BECKER is a cost estimating program, DESIGN 3 is a one dimensional MHD generator design program, and NASA SP-273 is a thermochemical equilibrium program.

The conceptual power plant model, and hence the modelling code, require constant updating to remain viable tools in predicting the performance and cost of electricity for MHD/steam combined cycle systems. Updating the code is required to keep current with developing technology to ensure use of better process modeling techniques and/or use of formulas derived from the ever increasing number of empirical performance relationships. For example, in the present configuration the MHD channel modelling incorporated in the DESIGN 3 subroutine was replaced with a subroutine entitled CHAN to reduce computer run time. In subsequent paragraphs, an overview of the current SYSTEMS model will be provided--with component analysis--and the interactions of the main program SYSTM and the subroutines SINGH, BECKER, CHAN, and PRESTO II described. Results obtained from the extended model is the foundation for the natural gas fired MHD/steam combined cycle analysis presented in Chapter IV.

The MHD Combined Cycle Power Plant Model

While MHD electrical power generation is highly efficient over its generator channel length, as a stand-alone power generating source the overall efficiency would be extremely low. The MHD channel exhausts a considerable amount of waste heat which is capable of producing steam for conventional power generation. Using less than the full combustion energy for power generation lowers the possible cycle efficiency, since the value of the high temperature reservoir has decreased. By combining the MHD generator with a conventional steam plant the overall efficiency exceeds each respective stand-alone efficiency. The MHD components can be arranged on the front end of a combined cycle power plant and are conventionally called the topping cycle components. The conventional steam power plant components, operating on the exhaust products from the topping cycle, are conventionally called the bottoming cycle components.

The MHD/steam combined cycle power plant modeled in the SYSTEMS code is comprised of the high efficiency MHD topping cycle and the conventional steam bottoming cycle. Figure 3 illustrates the interconnections between each of the following topping cycle components: the primary combustor, the nozzle, the MHD channel, the superconducting magnet, a DC/AC inverter, the first stage diffuser, the high temperature air heater (HTAH), the intermediate temperature air heater (ITAH), and a primary combustion air compressor. The modeled bottoming cycle, illustrated in figure 4, consists of both conventional steam plant components and a simulated steam source. The major steam plant components are: 6 steam turbines (1 high, 1 intermediate, and 4 low pressure), 4 feedwater heaters, and a condenser.

The topping cycle is unable to efficiently produce electrical energy once the combustion gases have cooled below a temperature which supports adequate thermal ionization of the seed compound. This lower temperature for ionization is approximately 2000 K. This is the reason for combining the MHD plant with a steam plant. The high temperature exhaust gases are still capable of superheating steam for conventional steam turbine electricity generation. The topping cycle also supplies a considerable amount of heated water to the bottoming cycle. In the topping cycle, the water is heated while traversing the diffuser, MHD channel, nozzle, and combustor wall cooling sections. The heated water is formally converted to steam in the radiant furnace which utilizes the sub stoichiometric gas stream exhausted from the topping cycle, as illustrated in figure 4. The specific process of energy exchange between the topping and bottoming cycles is detailed in the following component discussions.

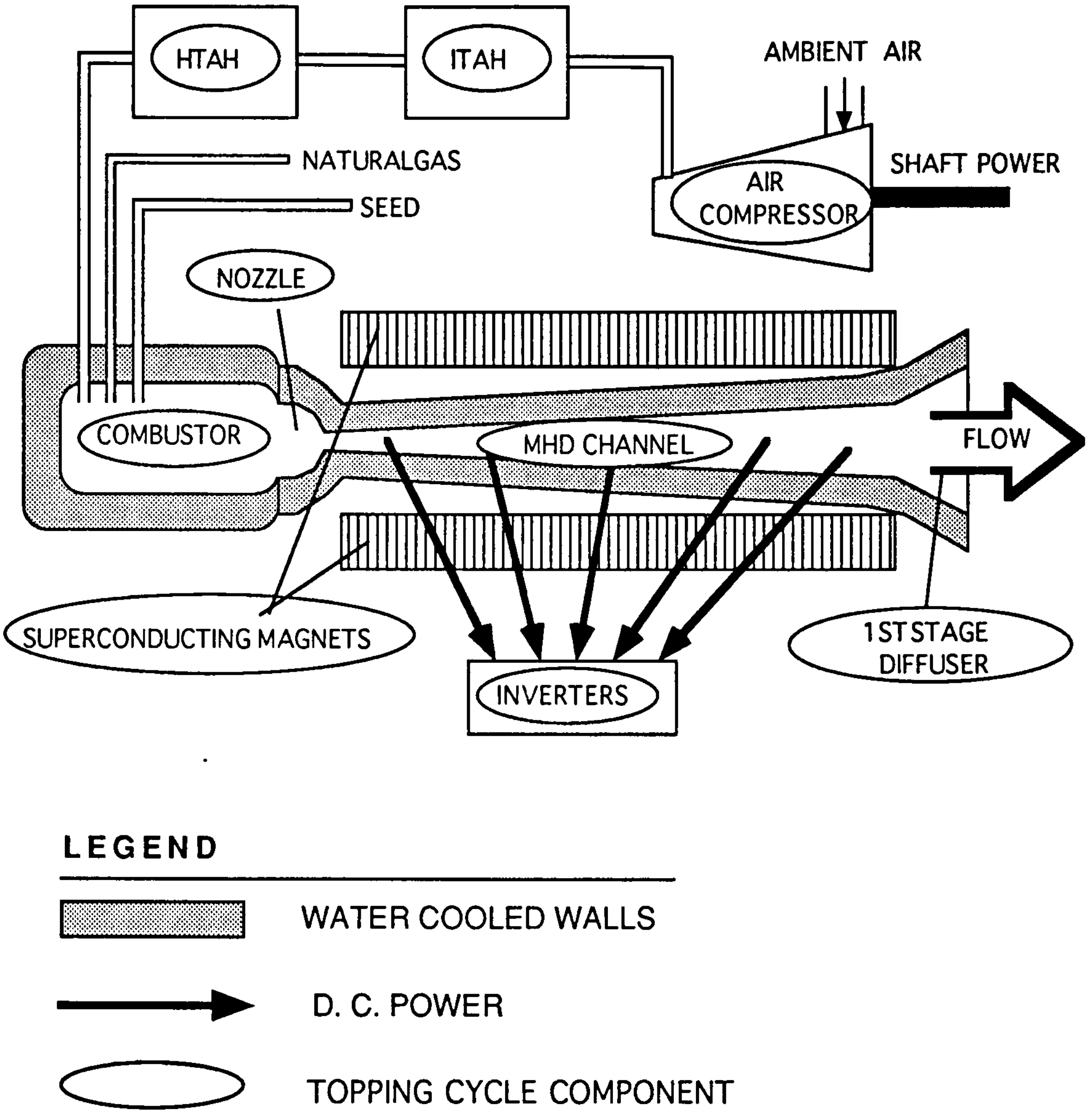

Figure 3. The Topping Cycle Model

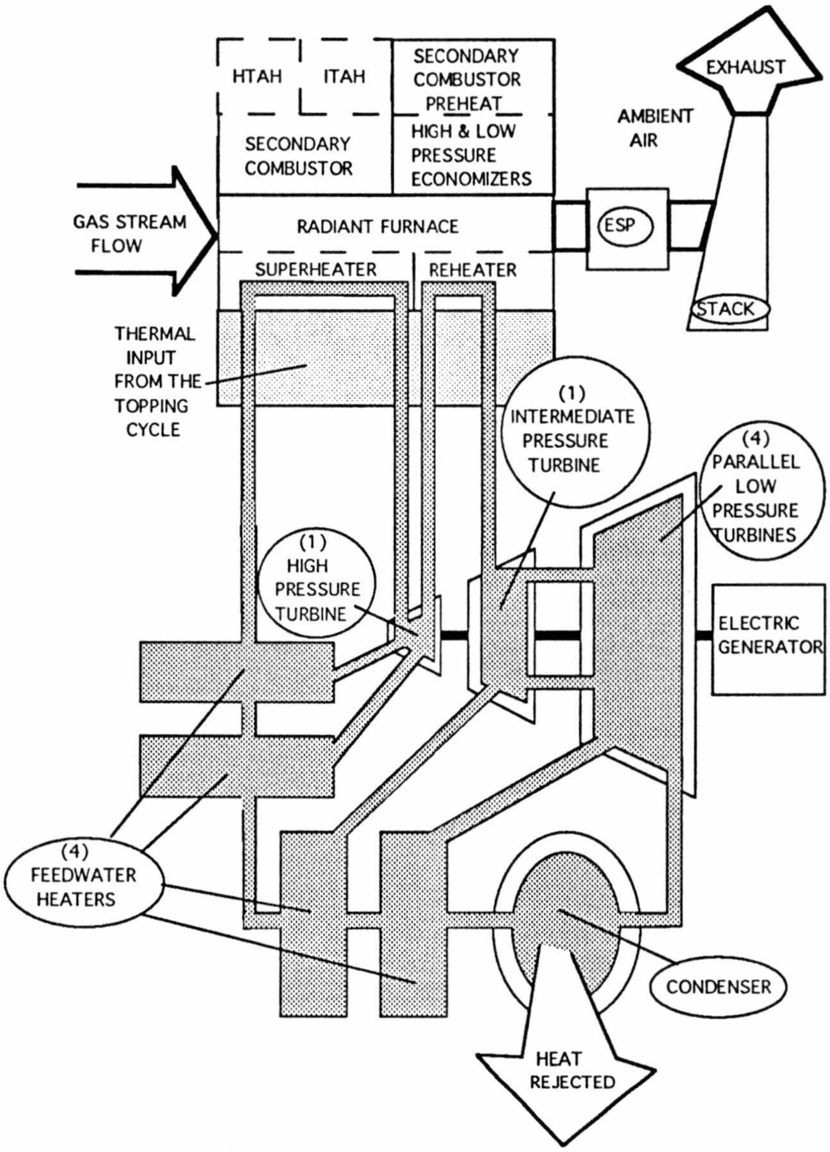

Figure 4. The Bottoming Cycle Model

The Topping Cycle

The first step for an open cycle natural gas fired MHD cycle is the production of the high temperature plasma. The combustion product properties are determined using the chemical equilibrium code NASA SP-273 located in the SYSTM code. The fuel type and flow rate, the air preheat temperature, the seed type and weight percent, the primary stoichiometry, the combustor pressure, and an assumed combustor heat loss value taken proportional to the reactant flow rate are each independent variables used to establish the primary combustor thermodynamic properties. The combustor heat loss variable has two functions, first it reduces the available energy in the combustor prior to the initial equilibrium calculations, and secondly the variable is later multiplied by the total reactant flow rate to establish a recoverable heat loss value. The heat loss variable used in this model was fixed at 4.94 cal/g to approximate an overall loss of 1% of the fuel thermal input, based on the higher heating value of natural gas. The resulting amount of recoverable energy transferred is considered to be substantial enough to additionally cover the recoverable nozzle heat losses. The recoverable losses are used later as a bottoming cycle thermal input source. While a 1% combustor/nozzle heat loss is somewhat optimistic, the value was assigned considering that heat loss percentage inversely relates to an increasing combustor size.

With the nozzle heat loss already accounted for in the combustor model, the gas flow was taken to enter an isentropic nozzle designed to obtain any Mach number specified by the input. The coded model allows for specification of either a constant plasma velocity or a constant plasma Mach number boundary condition in the MHD channel. For the present study the boundary condition of a constant 0.88 Mach number was specified. The subsonic value ensures that subsequent flow through the MHD channel will not involve a shock wave, as would be the case with a supersonic flow. A shock occurring in a MHD channel would reduce the possible power output consequential to pressure recovery losses associated with shock waves. Solutions to the nozzle equations, coupled with the known mass flow rates and Mach number specification, allowed for the calculation of the MHD channel entrance area.

The gas flow entering the MHD channel at this point is an ionized plasma with analytically determined thermodynamic and electrical transport properties. The MHD channel performance is based on a one dimensional, steady flow, and constant Mach number model. The model is enhanced with empirical formulas for use in estimating MHD channel response to heat loss, turbulent dissipation, and wall friction effects. The channel interactions are developed by numerically integrating the governing differential equations using a Runge-Kutta algorithm. The advance is terminated when the channel length reaches a maximum prescribed length of 20 meters in this model or when a pre-determined cutoff pressure of 1.05 atm total pressure has been attained. The maximum length constraint is consistent with both performance and economic feasibility. Regarding performance, the presence of a highly conductive plasma beyond 20 meters seems doubtful when considering both the channel wall cooling and the pressure reduction that results from the viscous effects associated with significant length over hydraulic diameter ratios. Economically speaking, beyond 20 meters length the superconducting magnet cost clearly makes the topping cycle capital prohibitive. The cutoff pressure of 1.05 atm is the minimum value that will ensure a near atmospheric pressure entering the radiant furnace following the water cooled diffuser section. After the MHD channel calculation, the MHD enthalpy extraction (MHD power output/the total power available), channel efficiency (MHD power output/the isentropic power available over the same pressures), channel heat loss, exit area, and exiting thermodynamic property values are known.

The combustion products are considered to enter two diffuser stages after exhausting the channel. Only the first diffuser stage requires distinct calculations in this model since the second stage diffuser is assumed to be essentially part of the radiant boiler. The first stage diffuser uses empirical correlations to determine the heat loss during the pressure recovery. The diffuser was taken to have a coefficient of performance (COP) of 0.7 for this model. The coefficient of performance is, by definition, the ratio of the static pressure rise across the diffuser over the inlet dynamic pressure and therefore represents the percentage of dynamic pressure recovery. From the known inlet conditions, the diffuser heat loss, and the provided COP the diffuser outlet conditions are able to be determined.

The Bottoming Cycle

Following the first stage diffuser, the spent plasma gases enter the radiant furnace. This furnace has three primary functions 1) boiling the feed water, 2) housing the HTAH surface, and 3) decomposing nitrogen oxide (NO_x) as the gas cools. The walls would typically be designed as a membrane tube boiling surface. The furnace is modeled as a volume large enough to provide at least two seconds of residence time for the combustion gases. During the two seconds residence time, the gases would cool to the desired secondary combustor inlet temperature, 1367 K (2000 deg F) used in this work, and more importantly, the NO_x could decompose to a very low value, typically 100 ppm. The volume would also house a ceramic tube HTAH to heat the pressurized combustion air to the desired pre-heat temperature.

The secondary combustion is modeled at this point as a specified enthalpy-pressure (HP) calculation. The program allows for taking into account that the composition of the oxidants for the primary combustor and the secondary combustor may be different, for example using oxygen enrichment. In the case of oxygen enrichment, the program determines the final composition based on a weighted average of the primary and secondary oxidant compositions. For this study, air was taken as the oxidant for both the primary and secondary combustion processes, although the air preheat temperatures and combustor pressures for the two combustion processes are different. The secondary combustor pressure is considered to be approximately 1 atm.

The outlet conditions for the secondary combustor are determined using a simple energy balance and the combustion gases are then forwarded to the secondary combustor air preheater and economizer sections. The economizer is normally the location for additional heat transfer to the steam plant feed water heaters and the secondary combustor air preheat. The only heat transfer process requiring calculation in this model is the secondary combustor air preheating and an inlet temperature of 1060 R is used for the secondary combustion calculations. The exhaust flow balance leaving the economizer is passed through a dry electrostatic precipitator and outlet to the atmosphere through an induced draft fan and stack. The final amount of thermal input to the steam plant for this parametric case study was determined by subtracting the necessary air heater energy from the usable energy available following the secondary combustion. The available energy in the economizer section is considered to be the enthalpy difference between the enthalpy at the economizer entrance and a reference enthalpy at the stack conditions, reduced by the energy used to preheat the secondary combustor's air supply.

To provide the necessary compressed air to the primary combustor, a steam turbine compressor is used. The necessary steam flow requirements are obtained by a multiple step process. First the compression power required is obtained by an ideal compressor formulas. Next the power required is adjusted for an assumed efficiency, and finally the power is used as an input parameter to the steam plant program. The required steam flow overhead for the compressor power is returned by the program.

Finding the ultimate bottoming plant power production is the next step in the computer based model. PRESTO II, a steam plant modeling program discussed in detail later, processes the provided thermal input and various prescribed components to best produce electrical power. With the physical model concluded, the SYSTEMS program uses several different stored parameters to determine the cost estimates associated with development of the modeled combined cycle power plant. The rest of this chapter details how the program units interact to properly represent the above outlined model, the subroutine interaction is illustrated in figure 5.

SYSTM - The Thermochemical Equilibrium Routine

The thermodynamic properties of a substance at any point in a system may be approximated using the knowledge of the chemical equilibrium compositions throughout the respective chemical system. Obtaining the equilibrium compositions, for different points in a complex chemical system path, requires many numerical computations. The chosen method of solution to these complex equations depends on the specified independent properties from which the other properties are to be derived.

NASA, in 1961, developed a chemical equilibrium program using both the Gibbs and Helmholtz free energy relationships. The physically measurable

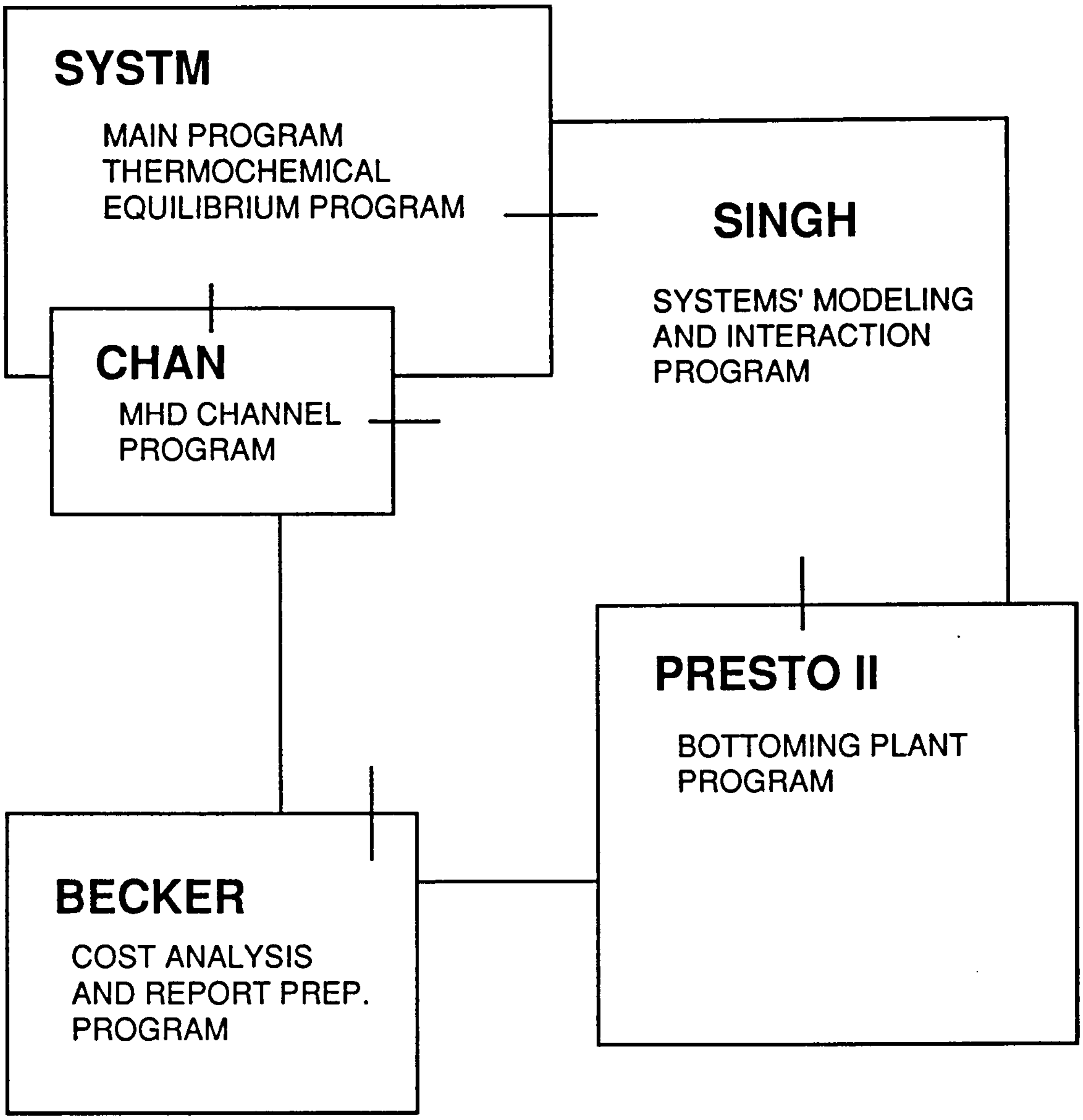

Figure 5. The SYSTEMS Code Interaction

properties of temperature and pressure or temperature and volume are both natural variables for the Gibbs and Helmholtz equations, respectively. Users of the initial program provided constructive feedback to NASA regarding the need for greater access to the program's subroutine units. Greater access to the subroutine units provided the opportunity to model thermodynamic processes with quick and efficient run times. Other program modifications included the improved management of condensed species and the new ability to account for ionized species. The updated chemical equilibrium code was designated NASA Special Publication SP-273. Individual subroutines of this code are used several times in a single system modeling run. The accuracy of the SYSTEMS' model relies heavily on the thermodynamic properties provided by the SP-273 program. The SYSTM code consists primarily of the NASA SP-273 code with a modified means of determining plasma ionization. The plasma ionization code was adapted to the program by Dr. L. W. Crawford, based on a paper submitted in 1961 to the *Journal of Applied Physics* by L. S. Frost (Chapman, 1977). While the "main" heading is located in the SYSTM code module, a significant portion of the power plant model and most subroutine interactions are performed from the SINGH subroutine discussed next.

SINGH - The Plant Performance Subroutine

The SINGH subroutine is the first subroutine called by the main program and, though modified, it still represents the plant systems' performance program. Each of the subroutines exchange most of their respective data through the use of common statements in their code. Only the SINGH code includes all of the common blocks used in the SYSTEMS program and thus, because of this interactive ability, is considered the heart of the program.

The SINGH subroutine is called after SYSTM code initialization. The SINGH code inputs the necessary topping cycle variables and calculates the thermal input and flow rates that comprise the topping cycle working fluid. The SYSTM code is then called, as if it were a subroutine, from SINGH to establish the initial working fluid properties at the primary combustor under the set initial conditions. Once the fluid properties in the combustor are calculated the isentropic nozzle equations are solved and the property values appropriately adjusted for a specified combustor nozzle exit Mach number. At the exit of the nozzle the SYSTM code is called again to calculate the thermodynamic composition of the plasma at the entrance to the MHD channel.

The code uses the known fluid flow rates and properties to calculate the MHD channel entrance area and then the CHAN subroutine is called. The specific calculations performed in CHAN will be discussed later in this chapter. The values returned by CHAN include: the generator enthalpy extraction, the channel efficiency, the channel length, the power produced, the exit area, and the two independent thermodynamic properties of temperature and pressure at the channel exit. Using the channel exit temperature and pressure, the other thermochemical properties and species composition are determined by another call to the SYSTM code. The available channel values for channel efficiency and power allow calculation of the overall channel heat loss based on an energy balance.

The SINGH subroutine, at this point in the code, calculates the air compressor power requirements for the specific combustor air pressure and mass flow conditions determined earlier in the code. The designated oxygen/fuel ratio, based on the input percent stoichiometry value, allows the required air flow rate to be calculated. Using ideal equations for an isentropic compressor, with an appropriate compressor efficiency adjustment, the temperature of the air leaving the compressor is determined. After the air exit temperature is fixed, the required thermal energy to heat the air to the designated air preheat temperature for combustion is determined from the static enthalpy increase from the inlet to the exit.

After the compressor power calculations, the SINGH program resumes following the modeled working fluid path. The fluid properties at the exit of the diffuser are calculated from the known diffuser input conditions and the assumed coefficient of performance for the diffuser. A specific geometry is calculated for this pressure recovery step and, based on empirical equations, the amount of heat loss through the diffuser is determined. The diffuser heat loss equations use the calculated diffuser dimensions for the evaluation.

The next computational step is for the secondary combustor inlet. Properties at this point are calculated for an input value of temperature and pressure. This permits the calculation of the amount of energy transferred to the feedwater in the radiant furnace by an energy balance. The secondary combustion outlet calculation is performed next by determining the amount of secondary air flow to achieve an overall stoichiometry of 105 %. The SYSTM code is used to provide the equilibrium concentrations and find the required oxygen/fuel ratio for the secondary combustion process. The code determines the thermodynamic values at both the specified economizer inlet temperature and the calculated stack temperature in order to determine the energy transfer in the economizer section. The secondary air heating energy exchange in the economizer section is accounted for by the drop in the enthalpy of the gas stream through the economizer.

At this point in the SINGH code, the topping cycle calculations are complete and the state point values for the primary combustor, the secondary combustor inlet and outlet, the economizer inlet and stack are available. By summing the heat loss terms associated with the primary combustor and nozzle, the MHD channel, the first stage diffuser, the available heat prior to the secondary combustor and the enthalpy rise from the secondary combustor to the stack and subtracting the required energy for the HTAH, ITAH, and secondary combustor air preheat, the thermal input to the bottoming cycle can be determined. Prior to calling the PRESTO II subroutine for bottoming plant performance calculations, the PRESTO II code is called to find the required steam mass flow to generate enough power to operate the primary combustor air compressor. Once the compressor steam mass flow rate has been identified, the bottoming cycle plant code is called and the steam mass flow adjusted prior to entering turbines. The last function of the SINGH routine is to call the cost estimating subroutine BECKER. The FORTRAN code of 1985, is available for review in the User's Manual for the UTSI MHD/Steam Power Plant SYSTEMS Code Topical Report referenced in the bibliography.

CHAN - The MHD Performance Subroutine

The CHAN subroutine is responsible for the MHD channel performance calculations. The calculations are based on coupled fluid dynamic and electrodynamic equations. The code uses several assumptions that simplify manipulations of the complex MHD governing equations. Only the solution for the mass, momentum, and energy conservation equations as well as for Ohm's law relations are necessary to evaluate the modelled MHD channel.

The generally accepted procedure for handling the interrelated equations is to apply several simplifying assumptions. Besides one-dimensional steady state flow, it is assumed that 1) the uniform magnetic field is in the z-axis direction only, 2) the gas velocity is in the x-axis direction only, 3) the current flux in the x-axis direction is zero (ideal Faraday design), and 4) semi-empirical relations are used for the loss terms. The reduced governing equations are presented below. The conservation of mass is expressed as,

$$\rho \; u \; A = \dot{m} \tag{3}$$

where $\dot{m}$ is the mass flow rate, and ρ, u, A are the plasma density, velocity and the flow cross section, respectively. The conservation of momentum is written as,

$$\rho u \frac{du}{dx} = -\frac{dp}{dx} - J_y B - \frac{4\tau_w}{d} \tag{4}$$

where additionally, p is the static pressure, $J_y B$ is the Lorentz force developed by the current flow in the plasma, τ_w is the viscous shear stress or frictional force at the channel walls, and d is the hydraulic diameter. The conservation of energy is given as,

$$\rho u \frac{d}{dx}\left(h + \frac{u^2}{2}\right) = J_y E_y - \frac{4u\tau_w}{d} + \frac{4\dot{q}_w}{d} \tag{5}$$

where h is the static enthalpy, and the three terms on the right account for Joule heating of the plasma, the rate at which the plasma does work against friction, and the heat transfer to the wall, respectively. Ohm's law is expressed as,

$$J_y = \sigma u B (1 - \Delta)(1 - K); \tag{6}$$

where σ represents the scalar conductivity, Δ is a lumped boundary layer dimensionless electrode voltage drop and K is a dimensionless loading parameter. The voltage drop factor, Δ, is more explicitly defined as,

$$\Delta \equiv \frac{V_d}{uBd} \tag{7}$$

used in this expression "V_d represents a lump loss term contributed by plasma nonuniformities (boundary layer), sheath drop and emission losses, current concentrations, as well as possible current leakage and shortings"(Wu, 1976). Lastly, K represents a dimensionless loading parameter given as,

$$K = \frac{V_T}{uBd(1 - \Delta)} \tag{8}$$

and represents the ratio of the output voltage to the open circuit voltage adjusted for the voltage drop. A short circuit loading would be represented by letting K equal 0 while the open circuit voltage would occur when K equals 1. The Faraday field is directly proportional to the chosen K value and from equation 6 the Faraday current is proportional to (1 - K). The available power is proportional to the product of the Faraday current and Faraday field values, and can be shown to maximize for a loading factor value of 0.5. However, certain material limits require that an adjustment from a loading value of 0.5 be made to ensure reliable and efficient operation. The maximum Faraday current allowed was set at 0.8 amps/cm^2 to ensure that electrode temperatures wouldn't be too great as a consequence of high current flow.

The maximum electric field allowed was set at 2000 volts to ensure that arcing wouldn't occur across the interelectrode gap between consecutive electrodes. With these constraints in mind the loading factor was assigned for each respective segment along the MHD generator channel. In the above equations u, B, E_y, and J_y, explicitly represent the plasma velocity, the magnetic field strength, the induced Faraday field, and the Faraday current in accordance with the earlier convention used in Chapter II. The shear stress and wall loss terms in the CHAN code are evaluated in the same manner as in the earlier referenced DESIGN 3 code.

After the assumptions have been applied to the MHD governing equations, the equations were reduced to a pair of coupled differential equations for pressure and enthalpy. A fourth order Runge-Kutta numerical integration technique was applied to determine properties between each step followed by a call to the SYSTM code at each step. The CHAN code fully integrates the governing differential equations by forward marching. Since the Mach number is fixed the differential plasma velocity is linearly related to the differential sonic velocity. The stepped differential plasma velocity can then be cast into the differential equations for pressure and enthalpy determination. This approach was compared to two alternative approaches, namely 1) assuming an ideal gas relationship in solving for stepped enthalpy values, and 2) calling the SYSTM subroutine to obtain the equilibrium properties during each Runge-Kutta step. The resulting data comparisons verified that the CHAN code, with the simplifications described, provided reasonable performance values at a much reduced run time in comparison with the second alternative.

PRESTO II - The Steam Plant Performance Subroutine

PRESTO is the name of a 1979 computer program developed by Oak Ridge National Laboratories (ORNL) from a General Electric code to evaluate the performance of regenerative superheated steam-turbine cycles. This program was used for an Environmental Protection Agency (EPA) report (report no. EPA-600/7-77-126) and claimed an accuracy of 0.1% in predicting net heat rates for General Electric in that report (Fuller and Stoval, 1979). In January 1982, this code was updated and labeled PRESTO II. This updated version, used as a subroutine in the system code, allowed the option of specifying performance based on shaft power required, total thermal input, or the required steam generator flow.

PRESTO II is used twice in the system code. The first call determines the amount of steam required to run the computed primary combustion air compressor turbine; while the second call, after removing the steam determined in the first call, performs calculations to determine the steam plant performance. The PRESTO II code provides the ability to specify external heat inputs either in parallel or series with the feed water heaters, before the steam generator, and directly following the condenser.

BECKER - The Economic Analysis Subroutine

The subroutine BECKER is predominantly comprised of an economic analysis program used in a 1977 University of Tennessee dissertation (Chapman, 1977). The code is based on several empirical relationships which, when evaluated together, provide the cost approximations necessary to predict the economic feasibility of a power plant. The code has undergone several modifications since its inception to ensure that the plant cost relationships remain current. BECKER, via, SINGH has access to all the program variables which together make up the plant model. The evaluation variables are different for each run because of the varying channel lengths, the changing thermal inputs to the steam plant, and the changing respective flow rates. Once the empirical costs are determined the program outputs the data in an easy to read economic analysis report shown in Table I. The components under the category heading in Table I are labeled numerically to correspond with the Federal Energy Regulatory Commission (FERC) indexing. The remaining column headings across the top are estimated plant construction costs. The component costs represent items that must be purchased from a specialty manufacturer or brought on site; conversely, the balance of plant (BOP) costs are the remaining items needed for a complete system (e.g. piping, valves, minor motors, etc.). The installation costs are the labor costs associated with setting up both the component and BOP equipment. The indirect costs include the engineering and architectural efforts required to design and construct individual items and structures. The contingency costs are for any unforeseen additional expenses that are not specifically included in the other column headings. Inclusion of a contingency cost is an accepted practice to realistically estimate projects of such magnitude. In the last column, the total for the combined expense of each respective component is listed.

Table I. A Typical Economic Analysis Report

ESTIMATED PLANT CONSTRUCTION COSTS
IN MILLIONS OF DOLLARS
FOR A 793 MWE PLANT

CATEGORY COMPONENT	COMPONENT COST	B.O.P. COST	INSTALLATION COST
310 LAND AND LAND RIGHTS	0.0000	2.7600	0.0000
311 STRUCTURES/IMPROVEMENT	0.0000	25.1272	19.7212
312 BOILER PLANT EQUIPMENT			
.1 COAL HANDLING	0.0000	0.0000	0.0000
.2 SEED HANDLING	0.8123	0.3412	0.3330
.3 RADIANT BOILER	10.6219	1.0303	6.3944
.4 STEAM GENERATION	114.4232	4.4049	29.5821
.5 EFFLUENT CONTROL	19.1753	4.6021	6.7113
.6 OTHER BOILER SYSTEM	5.9923	2.0374	2.9362
SUBTOTAL	151.0250	12.4159	45.9571
314 TURBOGENERATOR UNITS			
.1 TURBOGENERATORS	29.4936	0.0742	1.6760
.2 CONDENSER & AUXIL.	0.0000	2.5378	0.4513
.3 CIRCULATING H20 SYS	0.0000	8.8721	1.7744
.4 STEAM PIPING/VALVES	0.0000	10.9694	0.7313
SUBTOTAL	29.4936	22.4535	4.6330
315 ACCESSORY ELECTRIC	0.0000	12.9897	17.8939
316 MISC. PLANT EQUIP.	3.5858	0.5020	0.5164
317 MHD TOPPING CYCLE			
.1 COMBUSTOR & NOZZLE	3.5700	0.0268	0.1428
.2 MHD GEN & DIFFUSER	11.4404	0.7379	0.2288
.3 MAGNET	23.8139	0.6025	8.3349
.4 INVERTERS	34.8449	17.1785	17.1785
.6 SEED REGENERATION	0.0000	0.0000	0.0000
.7 OXYGEN PLANT	0.0000	0.0000	0.0000
SUBTOTAL	73.6692	18.5457	25.8850
350 TRANSMISSION PLANT	0.0000	8.1611	1.5669
SUBTOTAL	257.7737	102.9551	116.1735

Table I. (Continued)

CATEGORY COMPONENT	INDIRECT COST	CONTINGENCY	TOTAL
310 LAND AND LAND RIGHTS	0.0000	0.2760	3.0360
311 STRUCTURES/IMPROVEMENT	16.0627	8.0819	64.5538
312 BOILER PLANT EQUIPMENT			
.1 COAL HANDLING	0.0000	0.0000	0.0000
.2 SEED HANDLING	0.1987	0.2649	1.7883
.3 RADIANT BOILER	2.7070	3.6093	24.3630
.4 STEAM GENERATION	22.2615	29.6821	200.3539
.5 EFFLUENT CONTROL	4.0754	5.4339	36.6787
.6 OTHER BOILER SYSTEM	1.4658	1.9544	13.1922
SUBTOTAL	30.7085	40.9446	276.3762
314 TURBOGENERATOR UNITS			
.1 TURBOGENERATORS	3.4727	4.6303	31.2542
.2 CONDENSER & AUXIL.	0.3996	0.5327	3.5960
.3 CIRCULATING H20 SYS	1.4231	1.8975	12.8080
.4 STEAM PIPING/VALVES	1.5640	2.0854	14.0763
SUBTOTAL	6.8594	9.1459	61.7346
315 ACCESSORY ELECTRIC	6.5618	5.4682	39.3708
316 MISC. PLANT EQUIP.	0.3282	0.4431	4.8742
317 MHD TOPPING CYCLE			
.1 COMBUSTOR & NOZZLE	0.5609	0.7479	5.0484
.2 MHD GEN & DIFFUSER	1.8611	2.4814	16.7497
.3 MAGNET	4.9127	6.5502	44.2142
.4 INVERTERS	10.3803	13.8404	93.4226
.6 SEED REGENERATION	0.0000	0.0000	0.0000
.7 OXYGEN PLANT	0.0000	0.0000	0.0000
SUBTOTAL	17.7150	23.6200	159.4349
350 TRANSMISSION PLANT	1.3489	1.7986	12.1403
SUBTOTAL	79.5845	89.7782	621.5208
ENGINEERING SERVICES			79.3041
TOTAL ESTIMATED OVERNIGHT CONSTRUCTION COSTS			700.8249
CONSTRUCTION PERIOD -YEARS			5.65
TOTAL ESTIMATED COST INCLUDING INTEREST & ESC DURING CONST IN 1991.5 DOLLARS			772.7648

NOTE: ESCALATION AND INTEREST ARE BASED UPON AN ESTIMATED 5929085. MAN HOURS OF LABOR REQUIRED

The steam plant component costs are adjusted for inflation based on factors from *The Handy-Whitman Index of Public Utility Construction Costs,* while the remaining component and all BOP costs were determined using relationships established in the ECAS report. The installation costs were developed using various percentages of the respective component costs. Combining the component, BOP, and installation costs allowed for both the indirect and contingency cost determinations. The indirect costs were mostly assumed to be 15% of the above sum while the contingency costs were fixed at 20%, in accordance with conventional estimating practice, to assure a fair cost representation. The engineering services value found at the end of table I was obtained by multiplying the indirect cost subtotals by various factors to account for the different task relative loads. The overnight construction is obtained by summing the total column. This value represents the amount of money that would be required to hypothetically produce a power plant instantaneously. The construction period is determined using the empirical relationship presented in the ECAS phase II report (qtd. from Chapman, 1977). The total estimated cost including interest and escalation, accounting for the finite time required for construction, is based on the amount of time returned for the construction period. The analysis is conducted with the use of an assumed cash flow curve presented in the ECAS studies. Following the cash flow analysis, the resulting costs may be returned to the program in a prescribed equivalent year dollar amount.

The BECKER subroutine is called by the SINGH code after all the modeling calculations have been performed. The previously illustrated output data was instrumental in the power plant comparisons because each modeled power plant's economic viability was sensitive to the necessary material, construction, and operating costs. This subroutine was the backbone for evaluating the overall plant on an economic level. The final cost of electricity (COE) is dependent on the fuel costs and seed recovery efforts in addition to the operating and capital costs. The COE is defined as the sum of operating fuel, seed, and annualized capital costs divided by the product of the plant's rated annual power capacity and a respective capacity factor. The capacity factor represents the amount of time that the power plant can be assumed to be producing rated power over full-time operation. For this study a capacity factor of 0.65 was chosen, this is the same factor chosen in earlier economic analysis reports (Seikel and Harris, 1976 and Chapman, 1977). The fuel cost was fixed at an estimated $2.00/million BTU.

CHAPTER IV

PARAMETRIC ANALYSIS

To understand the economic viability of a natural gas fired MHD/steam combined cycle power plant requires both an evaluation model and a prioritized set of performance criteria. Use of the modified SYSTEMS program provided the method of analysis and, through parametric variations, generated the necessary data for the performance evaluation.

The most efficient way to study a function of several variables is to use parametric analysis. Parametric analysis is performed by fixing the most relevant variables, determining a base case model, then varying individual parameters to establish performance trends based on the respective individual parameters. Once the trends are understood a "best plant" design can be more efficiently sought by intelligent manipulation of the various parameters.

The parameters varied for the SYSTEMS study were: combustor air preheat temperature, combustor pressure, primary stoichiometry, and the seed percent based on relative weight. These variables were chosen because of their direct impact on the MHD channel entrance conductivity, and hence the channel efficiency and enthalpy extraction. The selected performance evaluation criterion were, listed by priority, the cost of electricity, the ratio of capital cost over plant power output, the overall plant efficiency, and the ratio of MHD power output over the total plant power output.

Once the parameters were chosen, the decision for a base power plant design was made. The midpoints of each parameter range were selected for use as the base plant model inputs. The following are the specific parameter midpoint values used: 1950K combustion air preheat temperature, 7 atm combustion pressure, 90 % stoichiometry, and 1% seed. The following paragraphs discuss the graphical results and provide interpretations for the results obtained for the different parametric variations.

Combustor Air Preheat Temperature

Varying the combustion air preheat temperature provided reasonable and justifiable results. For each of the selected evaluation criteria, increasing the preheat temperature increased the model plant's attractiveness. Figures 6 and 7 illustrate the significant reductions of cost of electricity and capital cost/power output respectively. Figure 8 illustrates the increase in the overall plant efficiency with an increase of air preheat temperature and figure 9 illustrates the increase in the portion of energy being produced by the MHD topping cycle.

The results above can be explained by considering a simple energy balance between the respective topping and bottoming cycles with their respective efficiencies taken into account. In a MHD/steam combined cycle power plant, some of the power produced in the bottoming cycle is required in the topping cycle. The bottoming cycle has a power producing efficiency of up to 40%, but only a portion of this power is for electricity production. The topping cycle efficiency can be as high as 93 %, and all the power produced is in the form of electricity. Recycling energy through the topping cycle, as opposed to the alternative of sending the same energy downstream to the lower efficiency bottom cycle, provides for higher efficiency and hence results in better overall plant performance.

The improved topping cycle efficiency was directly linked to the higher plasma conductivity at the channel entrance. For the fixed seed input of 1% by weight, the entrance conductivity to the MHD channel increased from 5.48 to

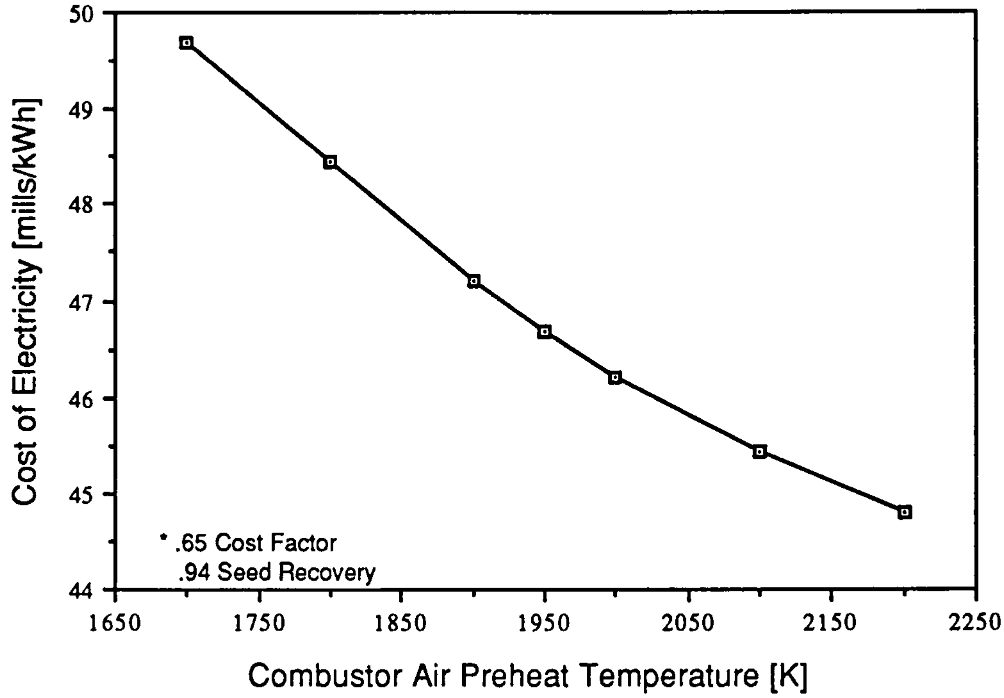

Figure 6. Cost of Electricity vs. Combustor Air Preheat Temperature

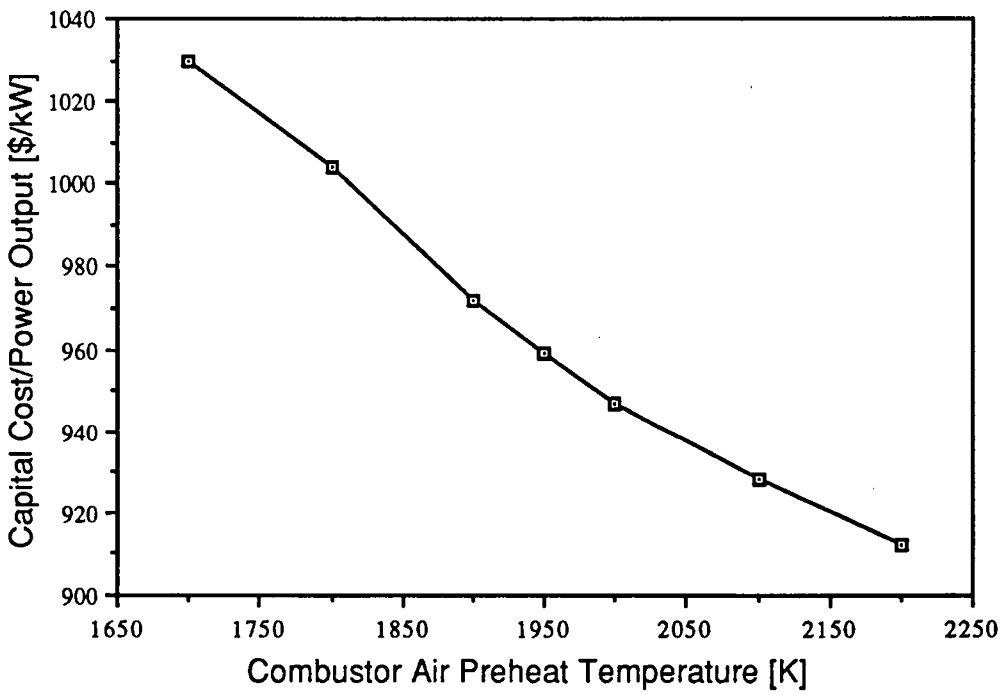

Figure 7. Capital Cost/Power Output vs. Combustor Air Preheat Temperature

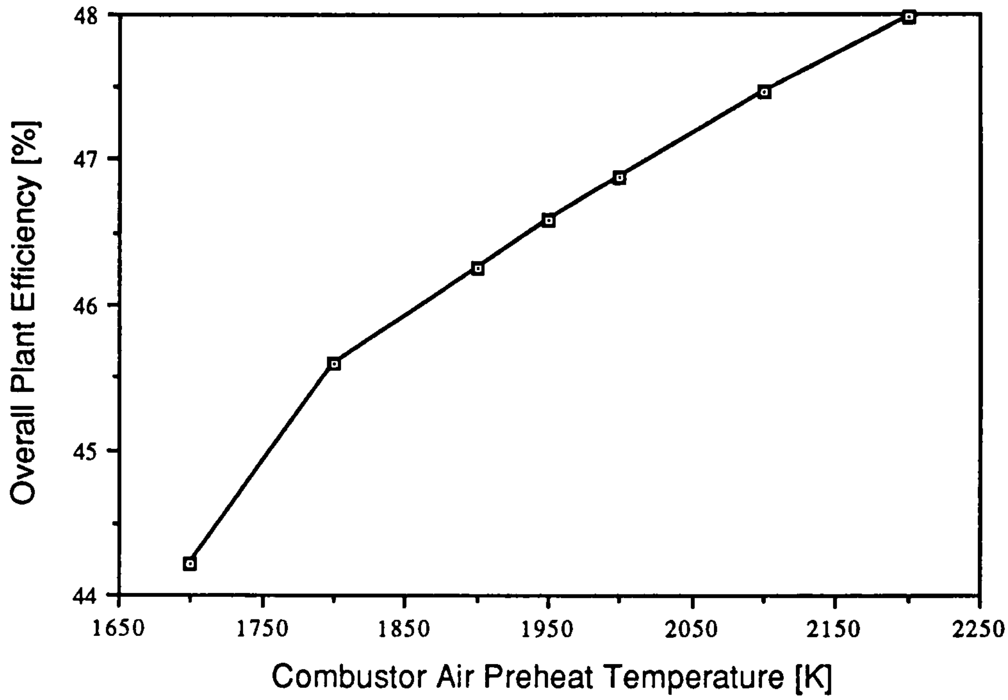

Figure 8. Overall Plant Efficiency vs. Combustor Air Preheat Temperature

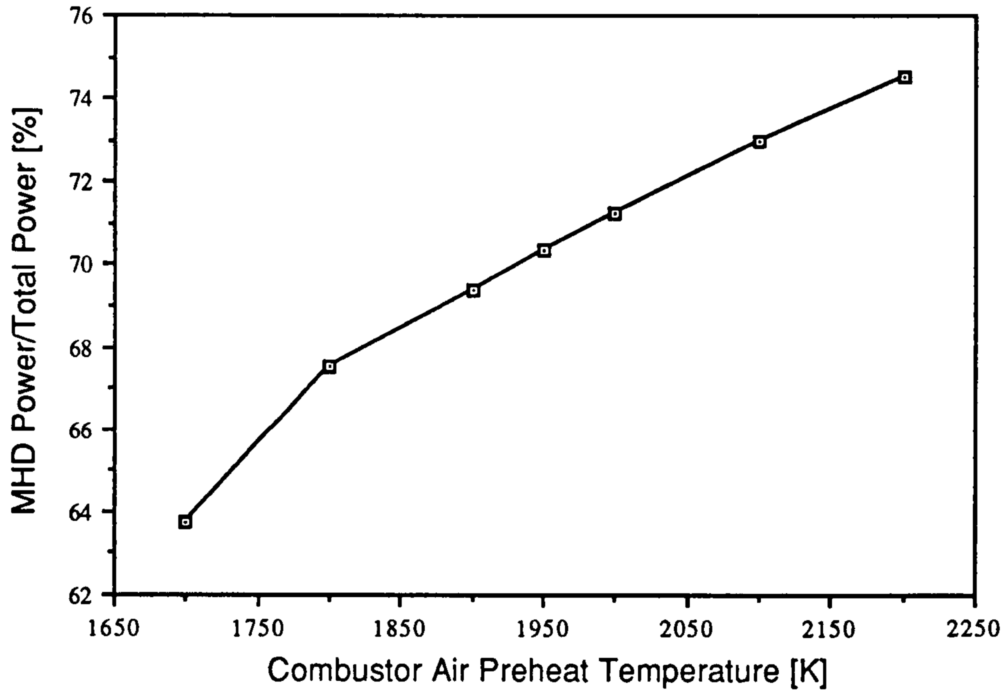

Figure 9. MHD Power/Total Power vs. Combustor Air Preheat Temperature

12.07 mho/m with the increase in preheat temperature from 1700 to 2200 K. This increase of entrance conductivity resulted in the channel efficiency rising from 84.38 to 88.34% over the same combustor air preheat temperature range. The channel efficiency is defined as the electrical power output ratioed to the drop of plasma enthalpy across the channel. The improved channel performance also had a direct factor in the reduced cost of electricity and capital cost. The resulting channel lengths, for the above cited runs, were decreased from 20.0 to 11.6 m over the same range of preheat temperatures. Reduction of MHD channel length in turn lowers the operating and capital costs significantly.

The only limitation to increasing efficiency, through temperature increase, lies in the availability of materials which can sustain the higher temperatures. An alternate method of increasing the combustion temperature is oxygen enrichment. The use of oxygen enrichment has two downsides; first a power consuming oxygen plant is required and secondly the mass flow through the higher efficiency channel for a constant thermal input is reduced. The use of an oxygen enrichment plant, which often can produce desirable results, was not assessed in this parametric analysis.

Combustor Pressure

Prior to discussing the graphical results, some background regarding pressure effects on the MHD channel need to be addressed. In the SYSTEMS code it can be shown that the MHD channel length is a function of entrance pressure for a specified exhaust pressure. The channel length becomes fixed after the pressure has reduced to a pre-selected cutoff pressure or the maximum length has been reached--whichever occurs first. Computation of the channel length, for a selected cutoff pressure, relies on the pressure ratio between the combustor pressure and the pre-selected diffuser inlet pressure.

Increasing the combustor pressure allows for a longer channel and accordingly MHD power extraction will occur over a longer distance; meanwhile, the longer channel length results in a greater temperature reduction and hence less energy for the bottoming cycle.

The variation of combustor pressure produced diverse results with respect to the four selected evaluation criterion. The cost of electricity and capital cost/power output graphs both indicate increasing costs with increasing combustion pressure as shown in figures 10 and 11 respectively. The trends were opposite to the earlier discussed combustor air preheat temperature graphs. The increased costs accompanying increased combustion pressure are associated with 1) additional compressor power requirements, 2) pricing associated with purchasing more and heavier duty plant equipment (especially the superconducting magnet), and 3) higher operating expenses required for an extended MHD channel. If the maximum length is reached prior to the specified diffuser entrance pressure, significant energy waste results.

The efficiency and MHD power/total power versus combustor pressure plots, figures 12 and 13 respectively, appear as parabolic curves peaking between 8 and 8.5 atm. The theory regarding a maximum point, in both figures 12 and 13, requires additional information regarding the trade-offs affecting overall plant performance. Increasing the pressure over the range indicated, reduced both the conductivity and the channel efficiency from 9.86 to 7.37 mho/m and 90.42 to 83.39% respectively. The greater combustor pressure also increased the channel length from 8.7 to 20.0 m. A longer MHD channel requires a longer more expensive superconducting magnet and exhausts a lower temperature resource to the bottom cycle. The multiple tradeoffs regarding pressure resulted in the value of 8 atm for the maximum power plant efficiency.

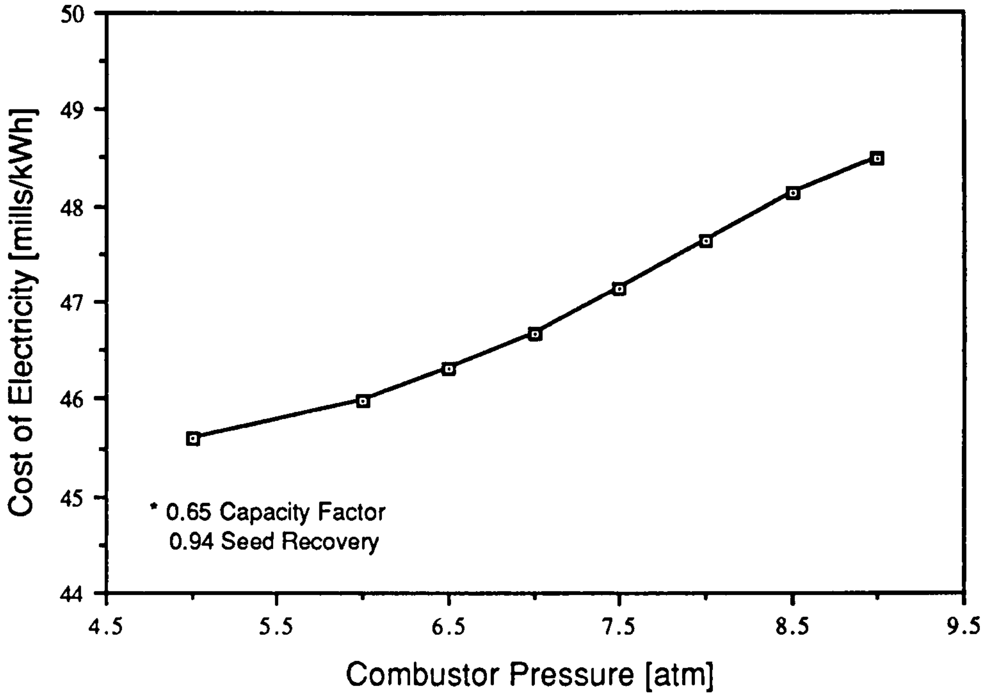

Figure 10. Cost of Electricity vs. Combustor Pressure

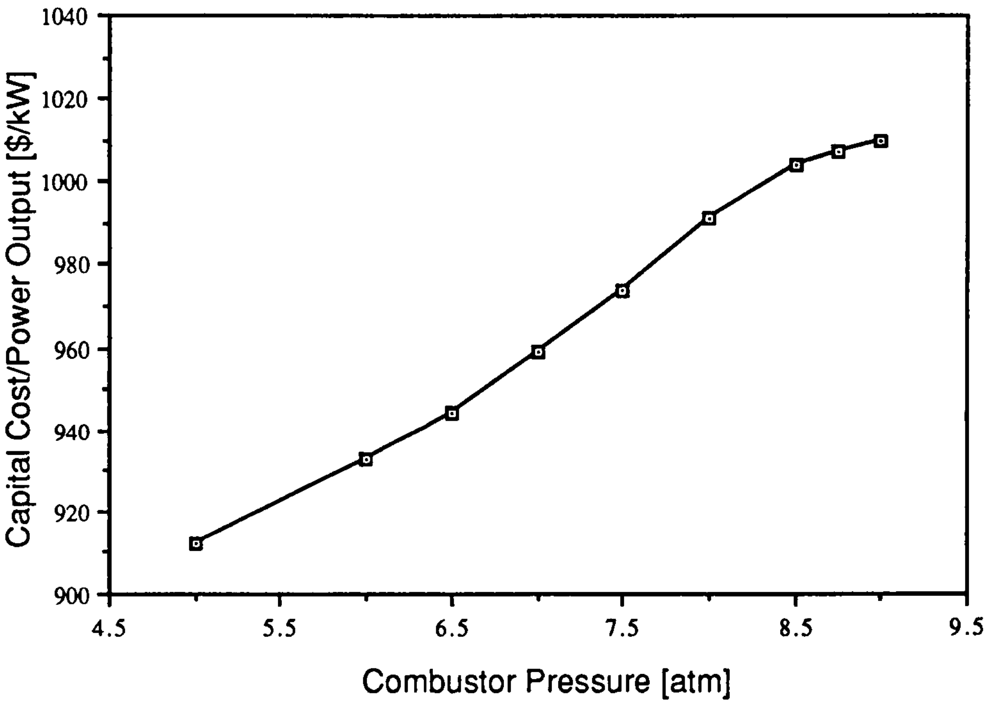

Figure 11. Capital Cost/Power Output vs. Combustor Pressure

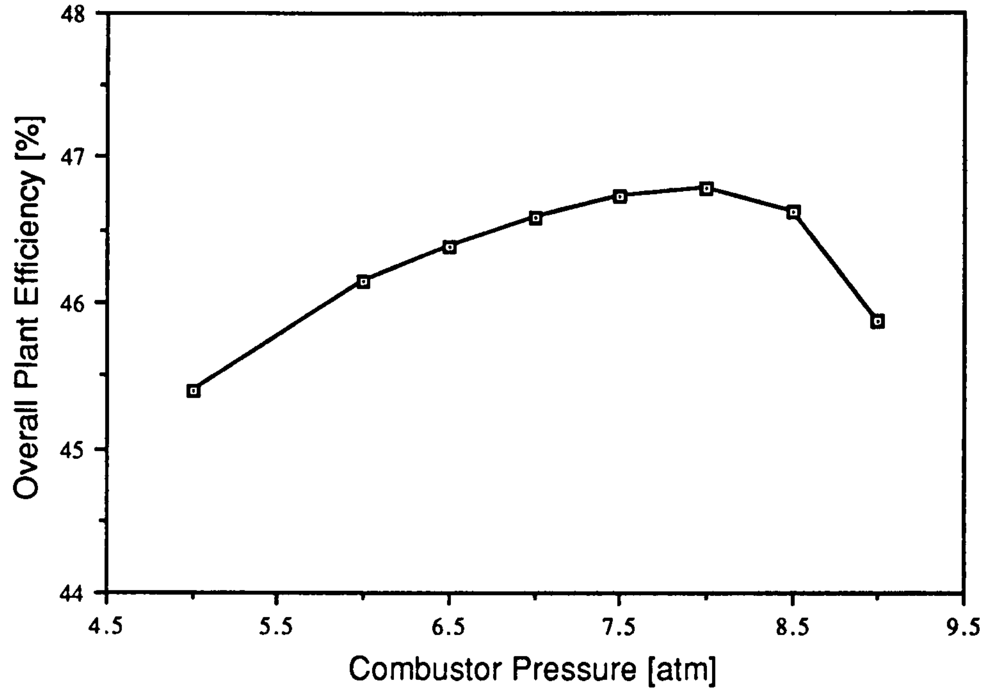

Figure 12. Overall Plant Efficiency vs. Combustor Pressure

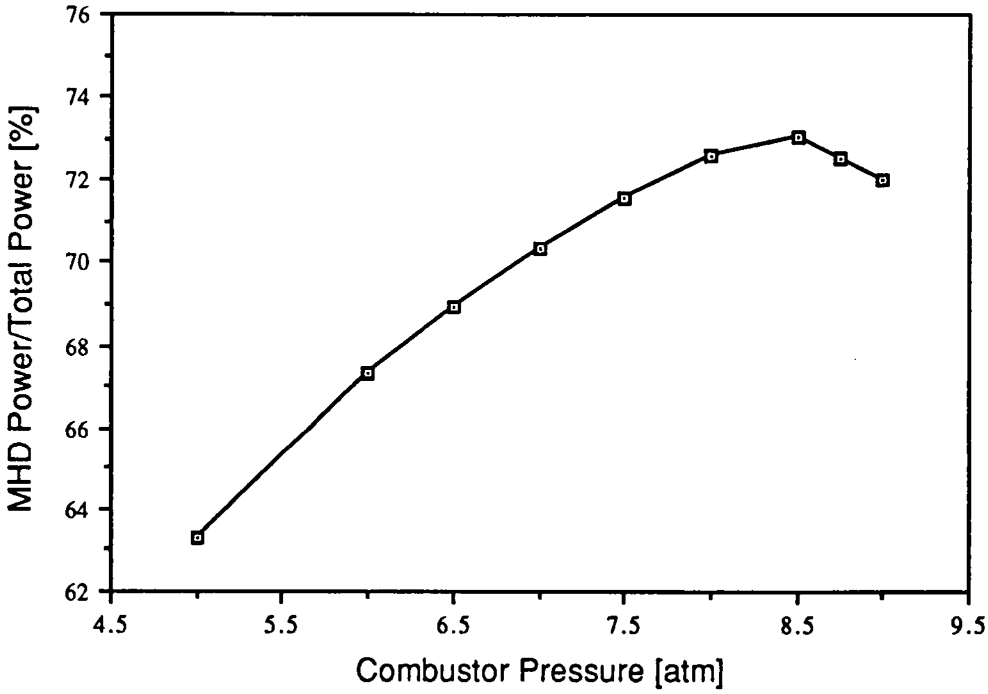

Figure 13. MHD Power/Total Power vs. Combustor Pressure

The combustion preheat temperature and combustion pressure exhibit opposite effects on the cost of electricity and capital cost ratioed to power output. Additional runs were performed to quantize the above costs as simultaneous functions of the combustion preheat temperature and combustor pressure. The results are shown in figures 14 and 15. In the figures it is possible to discern combinations of temperature and combustion pressure which have constant associated costs. For example, in figure 14, the combination of 1950 K temperature and 5 atm pressure has a cost of electricity of approximately 45.6 mills/kWh. Increasing the temperature to 2200 K and the pressure to 8.5 atm results in the same cost of electricity. On the other hand, starting at the same point in figure 15, at 1950 K and 5 atm, the capital cost ratio is approximatly 910 $/kW. Increasing the temperature to 2200 K, it is found that for the same capital cost the pressure can only be increased to 7 atm. This in turn illustrates that the cost of electricity and capital costs are not proportional.

Percent Primary Stoichiometry

Evaluation of the various percent stoichiometry graphs is best interpreted with a background of previous coal based studies (Chapman, 1979). The data of the previous coal fired MHD/steam combined cycle power plants suggests that: plasma conductivity reaches a maximum level near 85% primary stoichiometry, combustor temperature reaches its maximum at 88% stoichiometry, and the closer the percent stoichiometry moves toward unity the higher the resulting overall plant efficiency. Similar results were obtained for the present natural gas studies. The maximum electrical conductivity occurred at 89% primary stoichiometry, the maximum combustion temperature occurred at 92% stoichiometry, and again efficiency continued to climb as the stoichiometry percent approached unity.

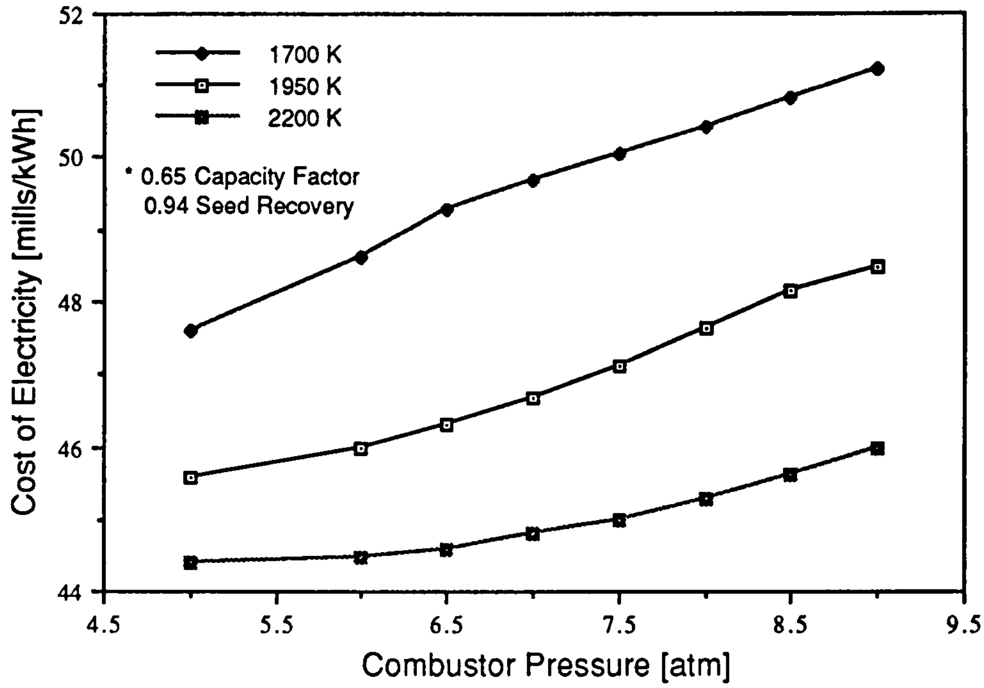

Figure 14. Cost of Electricity vs. Combustor Pressure
For Various Temperatures

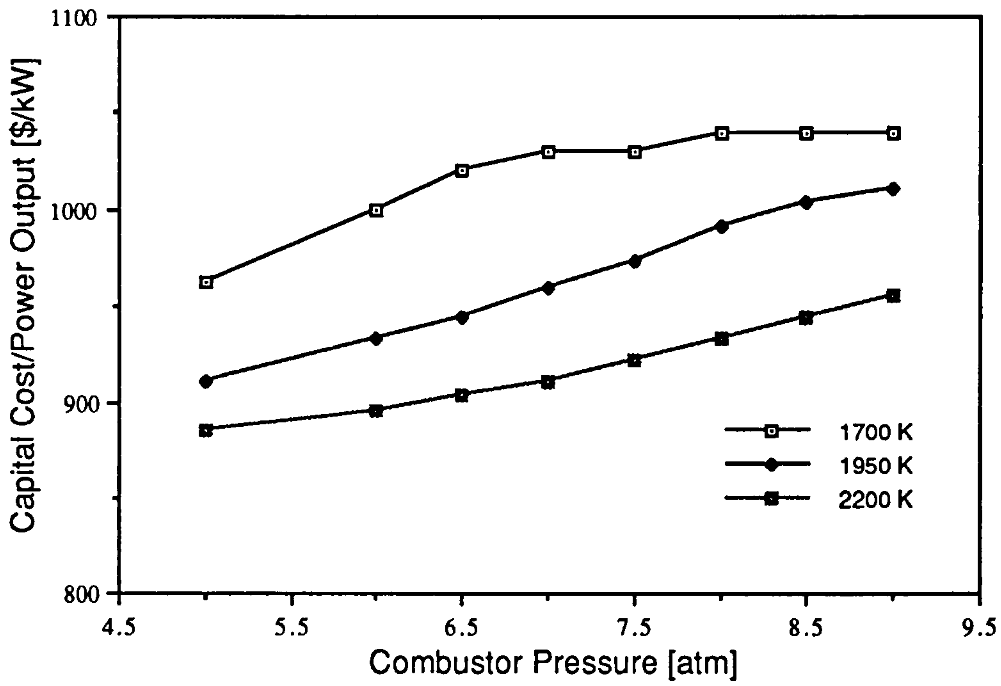

Figure 15. Capital Cost/Power Output vs. Combustor Pressure
For Various Temperatures

The best strategy for primary stoichiometry, concluded from the previous coal studies, is to maximize the stoichiometric value which ensures compliance with present day NOx emission standards. When both low cost of electricity and low capital cost/power output are considered as performance objectives, rather than maximum efficiency, an upper limit of 92% primary stoichiometry for natural gas is observed as the optimum value as shown on both graphs, figures 16 and 17. Therefore the final choice for the primary stoichiometry continues to be a value that restricts excessive NO_x; yet now, an upper limit of 92% primary stoichiometry exists for natural gas.

Increasing stoichiometry provides two major advantages. The first major advantage for increasing the stoichiometry involves the resulting increase in mass flow passing through the highly efficient MHD channel. This inherent advantage is significant enough to keep the overall efficiency curve on the rise even when the combustion temperature drops slightly at higher primary stoichiometry levels as shown in figure 18. The second advantage relates to the earlier discussed temperature effects. Namely, higher combustion temperatures are observed as primary stoichiometry is increased toward some upper limit, the value of 92% for natural gas. The higher efficiencies and greater mass flows are responsible for the positive slope seen in figure 19, representing the greater percent of topping cycle MHD power being produced, relative to the bottoming cycle.

Percent Seed

Variation of the percent seed parameter produced minimal plant-wide effects. The positive effects included a reduction of the generator channel length and a slight increase in channel efficiency. On the negative side, the increase in seed reduced the combustion and channel entrance temperatures.

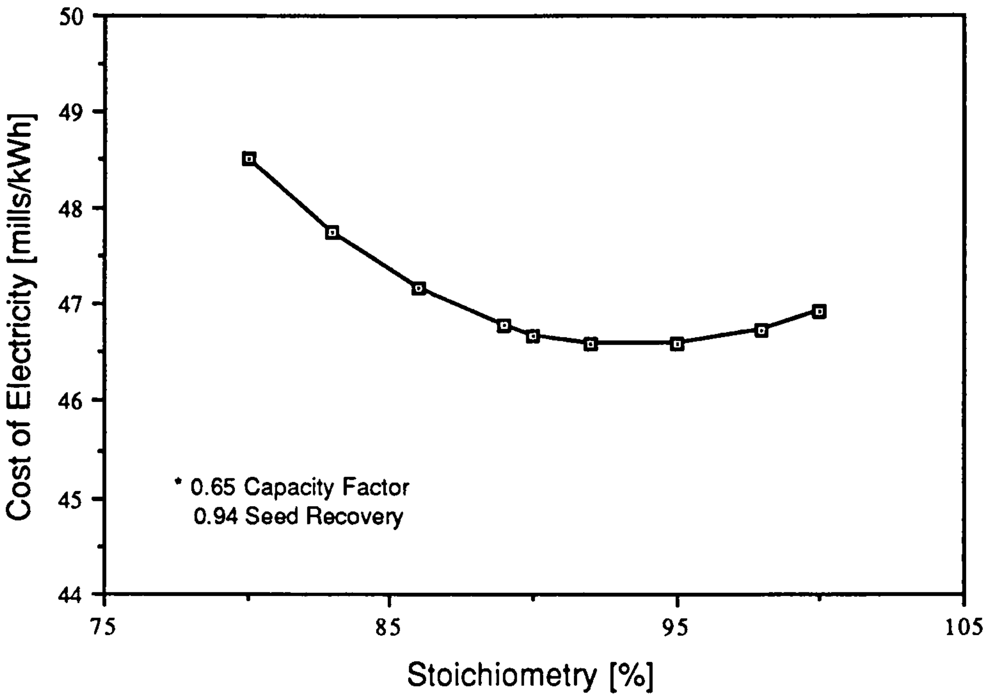

Figure 16. Cost of Electricity vs. Percent Stoichiometry

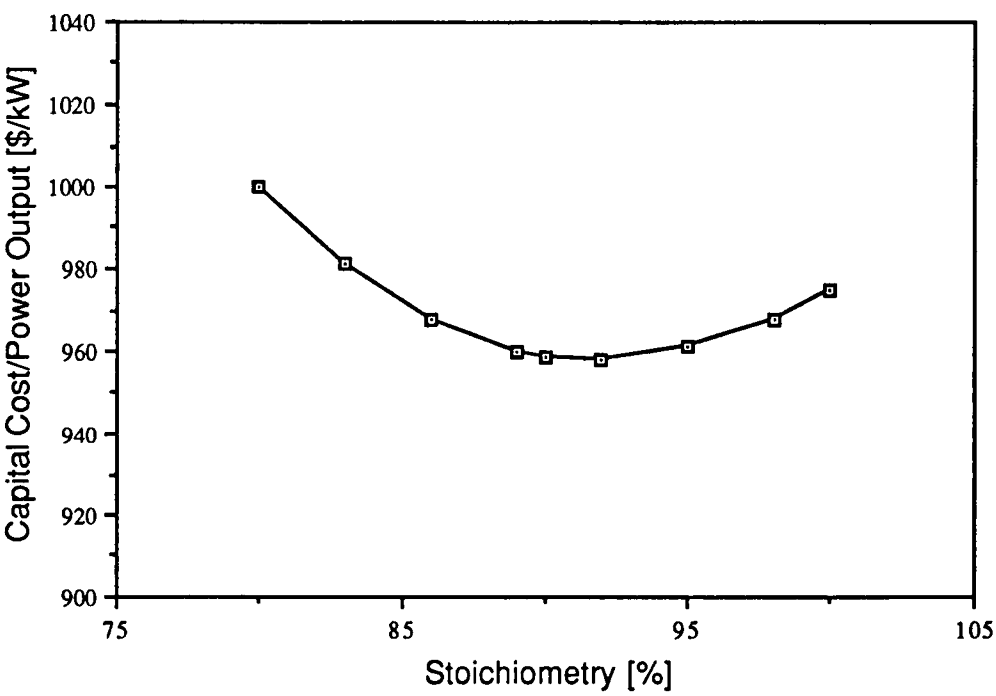

Figure 17. Capital Cost/Power Output vs. Percent Stoichiometry

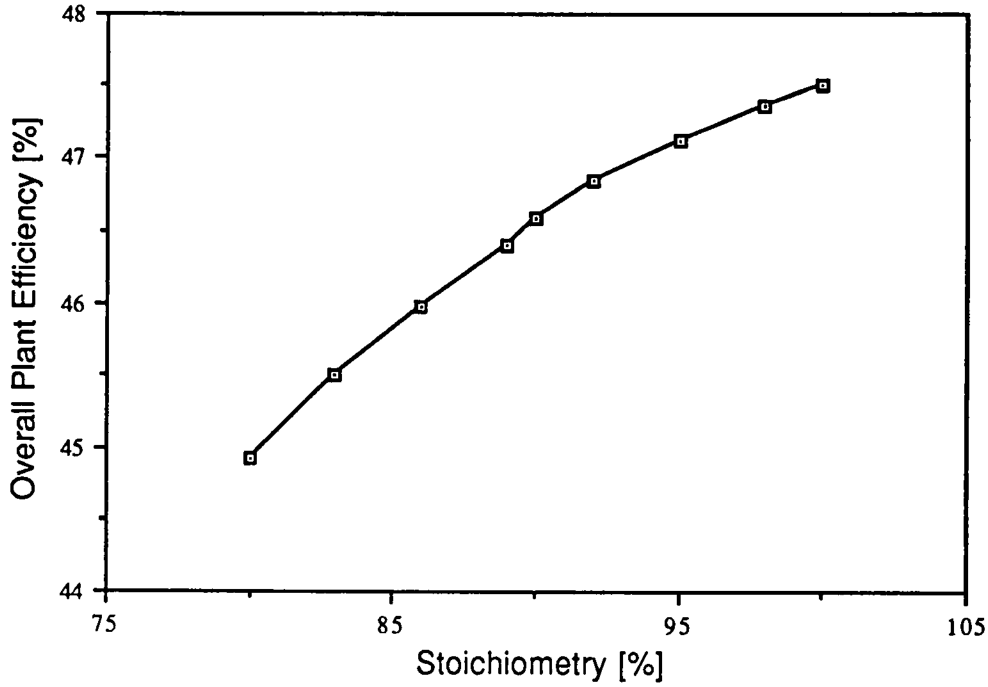

Figure 18. Overall Plant Efficiency vs. Percent Stoichiometry

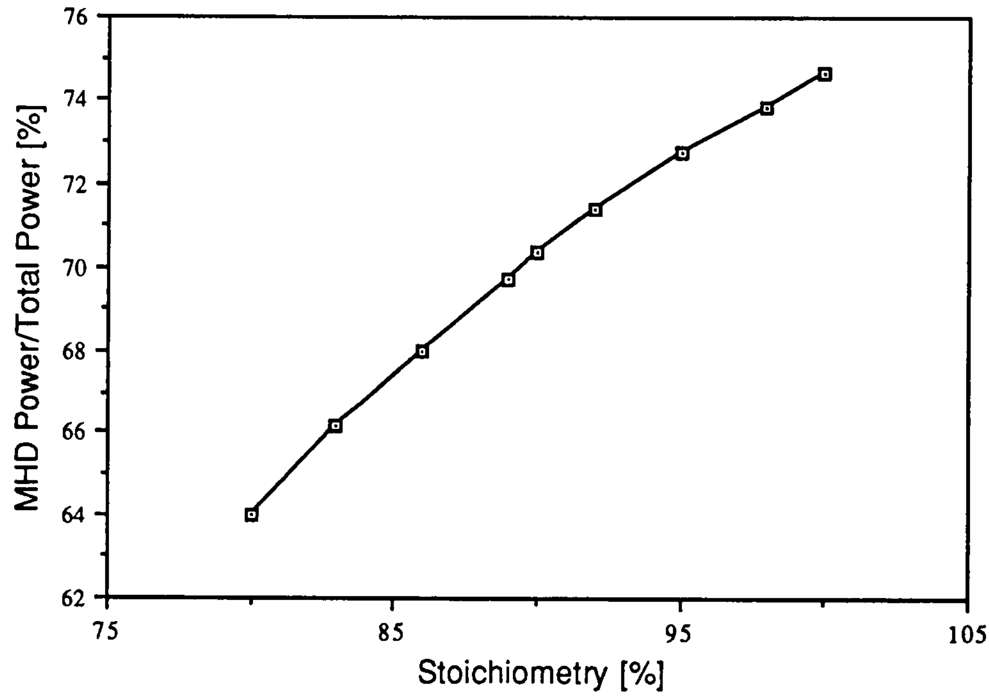

Figure 19. MHD Power/Total Power vs. Percent Stoichiometry

The above noted positive effects are attributed to the increased levels of entrance conductivity, which are shown in figure 20. Increasing the relative amounts of easily ionized potassium salt, produced and even greater increase in entrance conductivity. However, there is a diminishing rate of return as increases in the seed percentage results in proportionally smaller incremental increases in the plasma conductivity. The negative effect of temperature reduction can be attributed to the increased mass which acts as a thermal sink in the combustor. The cost of electricity graph, figure 21, plots the economic impact of the above stated pros and cons with respect to the increased percent seed. The cost of electricity graph illustrates an obvious minimum value at the 1% mark. Similarly, the capital cost/power output graph of figure 22 reacts to the increasing seed in the same manner, except for a skewed minimum to 1.2%.

Because of the decrease in available energy exiting the channel, the bottom cycle power plant efficiency also decreases. In total, the net power output for the combined cycle power plant is lower for the increased seed inputs resulting in the negatively sloped plot of overall efficiency vs. seed percent as shown in figure 23. Finally, figure 24 illustrates the percentage of power produced by the topping cycle. Clearly, within the range studied, the percent seed has a minimal effect on the percentage of power that the topping cycle provides.

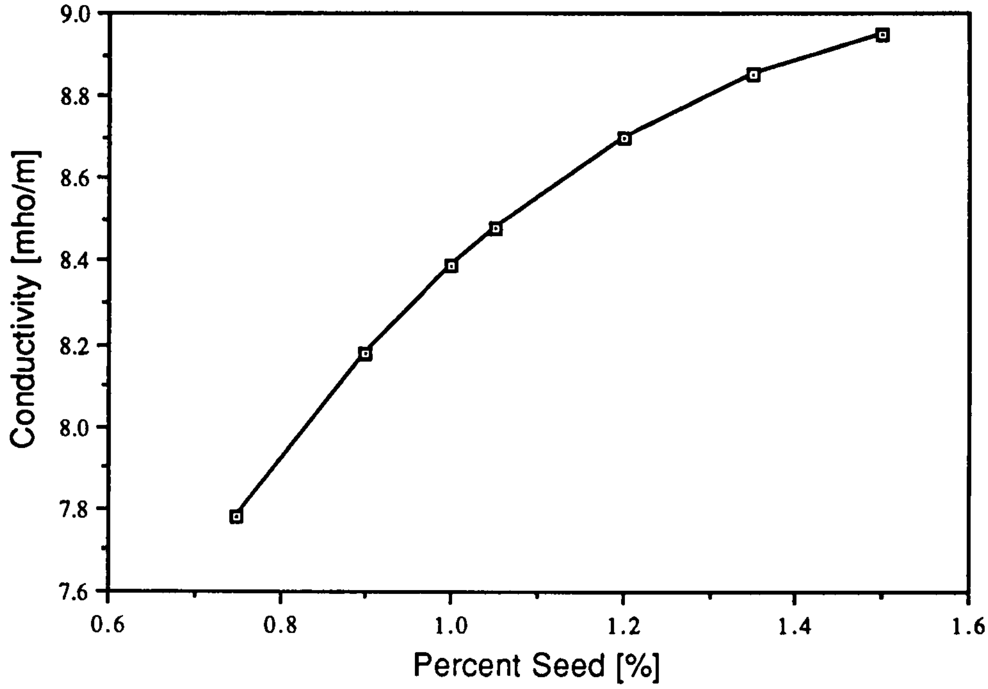

Figure 20. Conductivity vs. Percent Seed

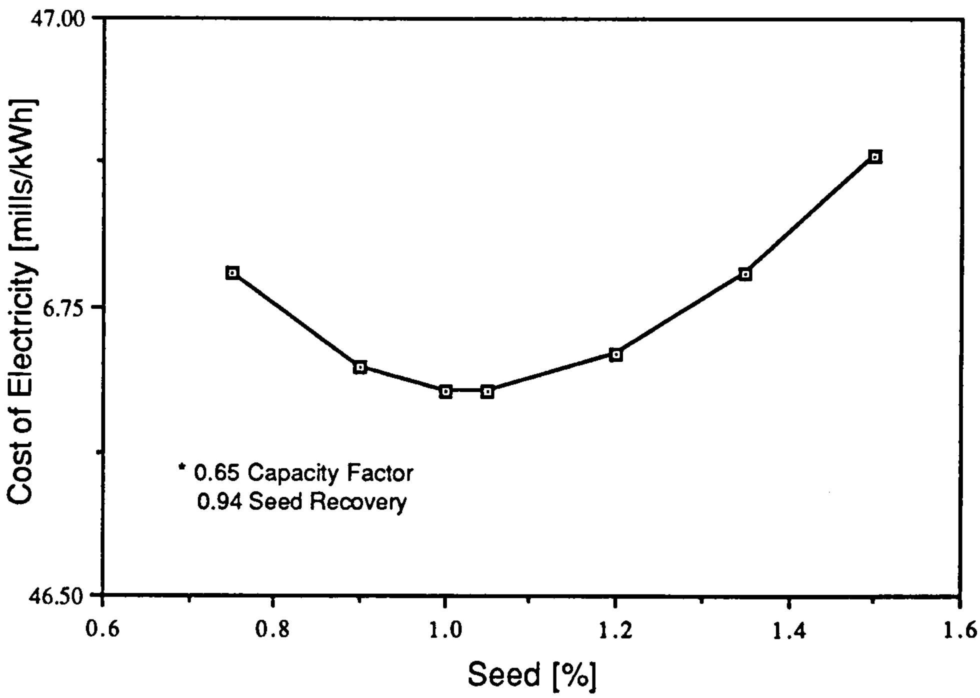

Figure 21. Cost of Electricity vs. Percent Seed

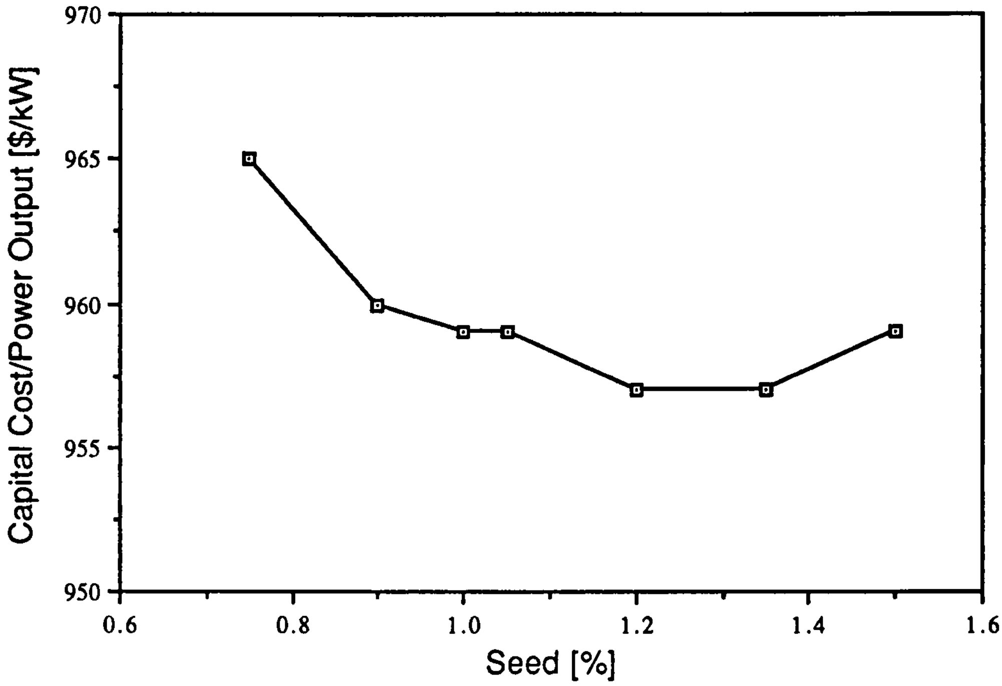

Figure 22. Capital Cost/Power Output vs. Percent Seed

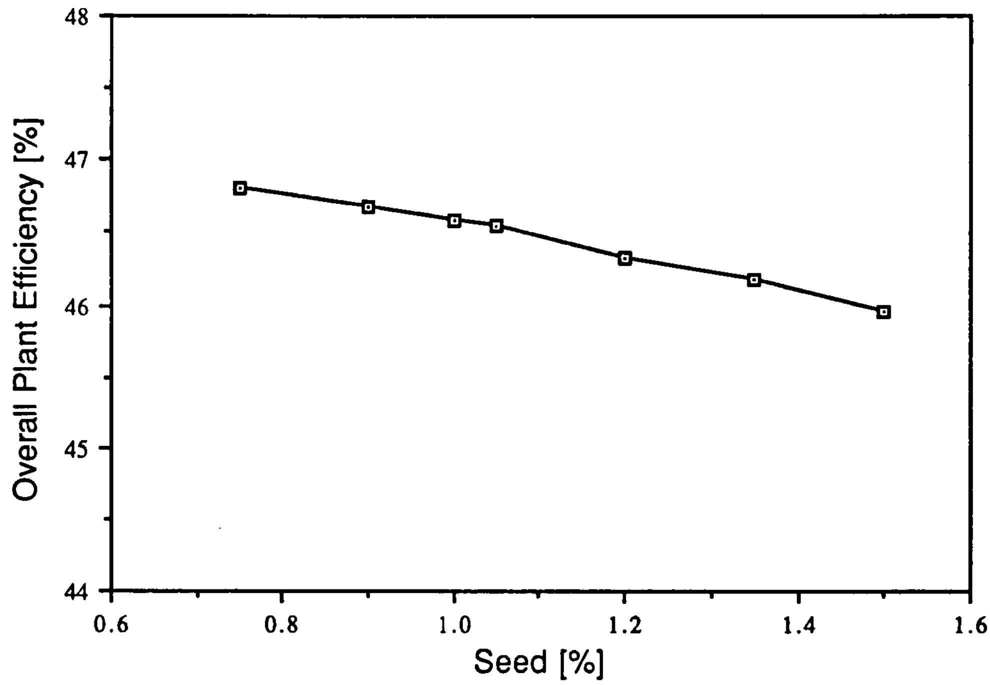

Figure 23. Overall Plant Efficiency vs. Percent Seed

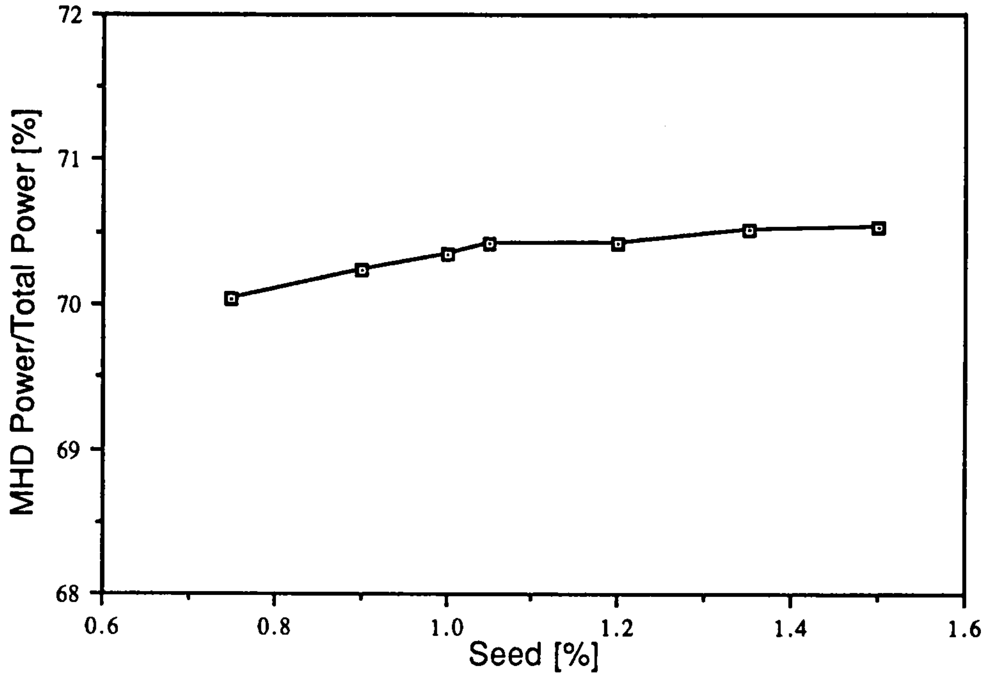

Figure 24. MHD Power/Total Power vs. Percent Seed

CHAPTER V

BASE PLANT SUMMARY, CONCLUSION, AND RECOMMENDATIONS

Summary of Best Plant Results

For each of the variables discussed in Chapter IV, optimum values were cited for use in determining a best plant design when the lowest cost of electricity (COE) is the primary objective. The different parameter effects on the COE were fairly independent from one another and a best plant design was evaluated using each of the respective optimum values. The best plant input values chosen were specifically: 2200 K combustor air preheat temperature, 5 atm combustor pressure, 92% primary stoichiometry, and 1% seed. When this plant was evaluated with the SYSTEMS code it did indeed provide the lowest COE value compared to all of the previous runs, namely 44.38 mills/kWh. For the sake of perspective this COE value needs to be compared with other forms of energy production. According to information presented by the International Atomic Energy Agency, the cost of electricity production for coal, nuclear, oil, and natural gas sources are 48, 43, 81, and 61 mills/kWh respectively.

The final step for this economic analysis involved arranging the thermal input to the bottoming cycle power plant model in a more realistic manner. Rather than allowing the power plant to operate on all the thermal input, as if it were available for steam generation, the different recoverable heat loss items discussed in Chapter III were more properly used as feedwater heating sources. Use of thermal energy for feedwater heating only, reduces the total power producing abilities of the steam turbine power plant.

The resulting best plant topping and bottoming cycle models are shown in figures 25 and 26, respectively. In figure 25, it is illustrated how the thermal energy available from the natural gas is recycled back to the combustor by way of the compressor, ITAH, and HTAH. Following the extraction of 681 MW of DC power and 123 MW of recoverable heat loss to the water cooled walls, the gas stream still has 2530 MW of high temperature thermal energy to be input to the bottoming cycle. After adjusting for the inverter losses associated with converting a DC power supply to an AC power supply, the net electrical energy output from the MHD topping cycle is 660 MW.

Figure 26 shows the 2530 MW of thermal energy entering the radiant furnace for heat transfer to the conventional steam plant superheat and reheat sections. At this point the amount of energy that can be utilized for steam production is determined by subtracting the energy designated to enter the secondary combustor. The substoichiometric flow next enters the secondary combustor where the 1195 MW of primary combustor air preheat energy is removed. The gas stream is then diverted to the high and low pressure economizer section. In this section, energy is removed for secondary combustor air preheat and the balance of available energy is utilized for feedwater heating. The gas stream, upon leaving the economizer section, finally exits at the stack.

The bottoming cycle is responsible for providing both electrical energy and energy to the topping cycle. Of the 421 MW of power produced by the bottoming cycle steam turbine section, only 282 MW of power is useful electricity production. Furthermore, of the 2530 MW input to the bottoming cycle approximately 1200 MW is sent back to the topping cycle as primary combustion air preheat. The combined cycle releases approximately 1100 MW of thermal waste to the environment via the stack and condenser. In

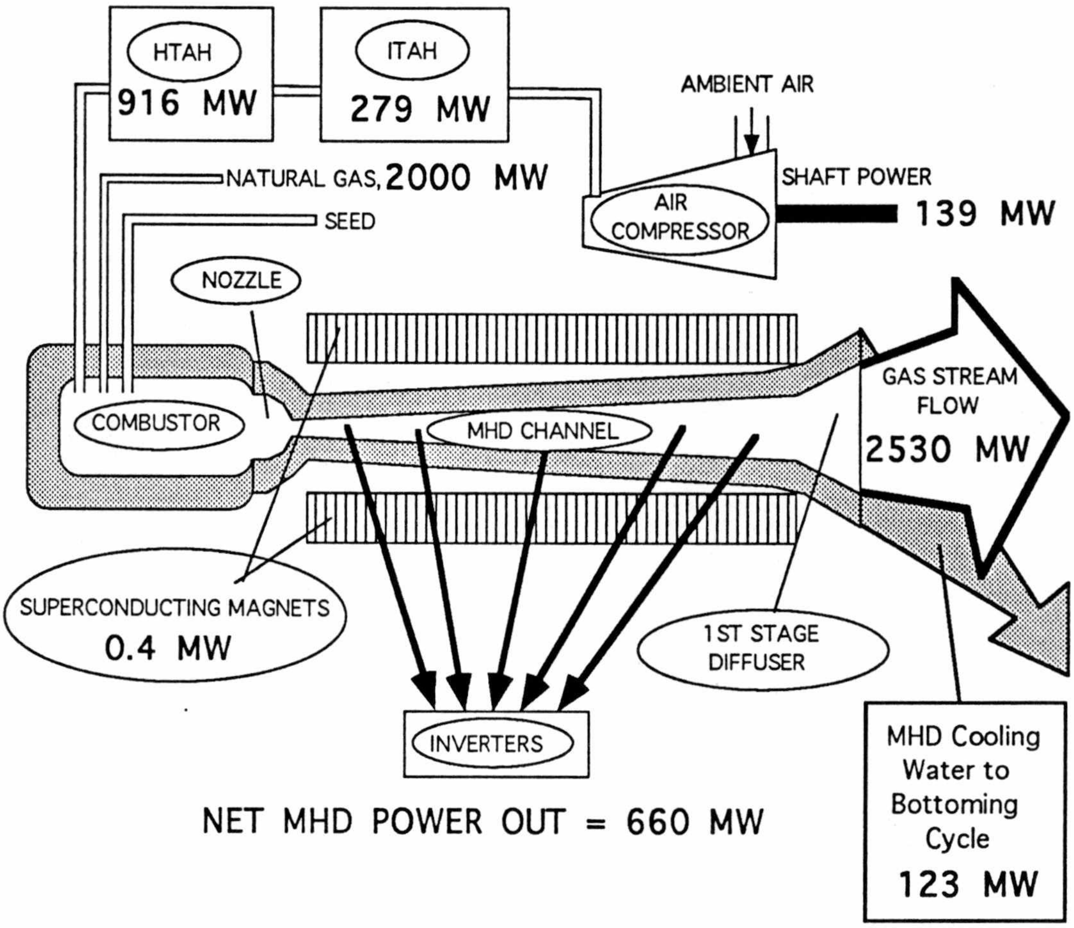

Figure 25. The Best Plant ModifiedTopping Cycle Model

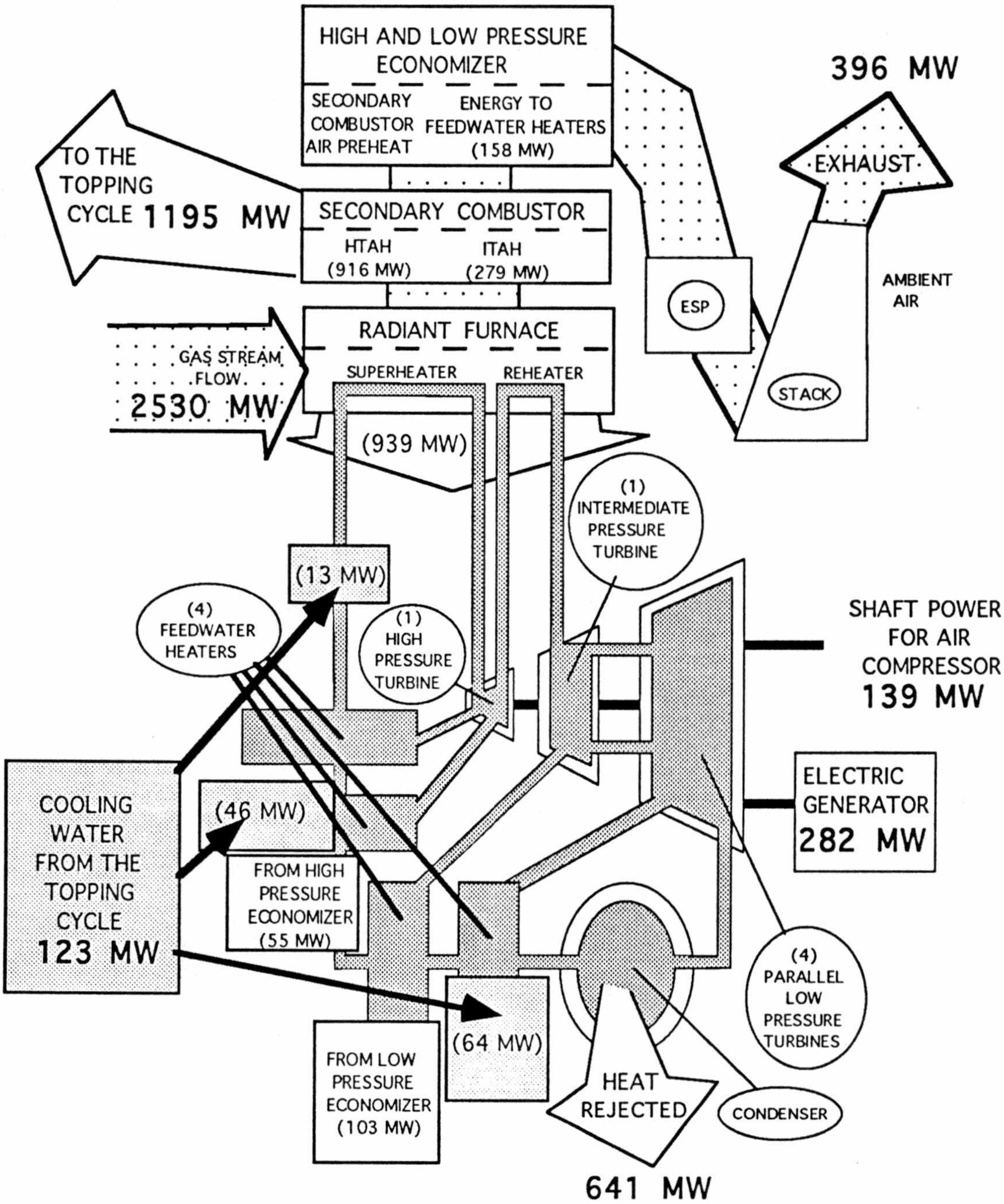

Figure 26. The Best Plant Modified Bottoming Cycle Model

comparison, a conventional power plant operating with a 35 % thermal efficiency would produce 1300 MW of thermal waste for a 2000 MW thermal input. The MHD/steam combined cycle inhibits the formation of harmful emissions through this controlled heat transfer between the topping and bottoming cycles.

The final model considered the combustor/nozzle heat loss to be the highest temperature source and the energy was input just prior to the bottoming plant steam generator. Additionally it was decided that any realistic MHD generator channel operation requires very cool inlet water to assure maximum cooling. The low temperature water is necessary since the water channels are located next to the walls of the generator and need to be as thin as possible to minimize the required magnet bore size. To meet this demand the heat energy was input parallel to the lowest temperature feedwater heater located just downstream from the condenser.

The remaining heat sources were input both parallel to the middle feedwater heaters and in series between them respectively. As was explained above, the power producing ability suffered when the thermal input was designated for feedwater usage. Specifically the bottoming plant steam cycle power output declined from 312.55 to 282.27 MW and the resulting COE rose to the value of 45.40 mills/kWh. Considering only the parameters studied, this is the best cost of electricity that can be obtained from the natural gas fired MHD/steam combined cycle power plant model. When compared with the earlier cited electricity generating costs for coal, nuclear, oil, and natural gas, 45.40 mills/kWh is most encouraging for further MHD system studies. The estimated capital costs report for the best plant configuration is provided in Table II for reference.

Table II. The Best Plant Economic Analysis Report

ESTIMATED PLANT CONSTRUCTION COSTS
IN MILLIONS OF DOLLARS
FOR A 904 MWE PLANT

CATEGORY COMPONENT	COMPONENT COST	B.O.P. COST	INSTALLATION COST
310 LAND AND LAND RIGHTS	0.0000	2.7600	0.0000
311 STRUCTURES/IMPROVEMENT	0.0000	25.1272	19.7212
312 BOILER PLANT EQUIPMENT			
.1 COAL HANDLING	0.0000	0.0000	0.0000
.2 SEED HANDLING	0.8123	0.3412	0.3330
.3 RADIANT BOILER	10.6219	1.0303	6.3944
.4 STEAM GENERATION	114.4232	4.4049	29.5821
.5 EFFLUENT CONTROL	19.1753	4.6021	6.7113
.6 OTHER BOILER SYSTEM	5.9923	2.0374	2.9362
SUBTOTAL	151.0250	12.4159	45.9571
314 TURBOGENERATOR UNITS			
.1 TURBOGENERATORS	29.4936	0.0742	1.6760
.2 CONDENSER & AUXIL.	0.0000	2.5378	0.4513
.3 CIRCULATING H20 SYS	0.0000	8.8721	1.7744
.4 STEAM PIPING/VALVES	0.0000	10.9694	0.7313
SUBTOTAL	29.4936	22.4535	4.6330
315 ACCESSORY ELECTRIC	0.0000	12.9897	17.8939
316 MISC. PLANT EQUIP.	3.5858	0.5020	0.5164
317 MHD TOPPING CYCLE			
.1 COMBUSTOR & NOZZLE	3.5700	0.0268	0.1428
.2 MHD GEN & DIFFUSER	11.4404	0.7379	0.2288
.3 MAGNET	23.8139	0.6025	8.3349
.4 INVERTERS	34.8449	17.1785	17.1785
.6 SEED REGENERATION	0.0000	0.0000	0.0000
.7 OXYGEN PLANT	0.0000	0.0000	0.0000
SUBTOTAL	73.6692	18.5457	25.8850
350 TRANSMISSION PLANT	0.0000	8.1611	1.5669
SUBTOTAL	257.7737	102.9551	116.1735

Table II. (Continued)

CATEGORY COMPONENT	INDIRECT COST	CONTINGENCY	TOTAL
310 LAND AND LAND RIGHTS	0.0000	0.2760	3.0360
311 STRUCTURES/IMPROVEMENT	17.8272	8.9697	71.6453
312 BOILER PLANT EQUIPMENT			
.1 COAL HANDLING	0.0000	0.0000	0.0000
.2 SEED HANDLING	0.2230	0.2973	2.0068
.3 RADIANT BOILER	2.7070	3.6093	24.3630
.4 STEAM GENERATION	22.2615	29.6821	200.3539
.5 EFFLUENT CONTROL	4.5733	6.0977	41.1597
.6 OTHER BOILER SYSTEM	1.6449	2.1932	14.8039
SUBTOTAL	31.4097	41.8796	282.6873
314 TURBOGENERATOR UNITS			
.1 TURBOGENERATORS	4.6866	6.2488	42.1792
.2 CONDENSER & AUXIL.	0.4484	0.5978	4.0353
.3 CIRCULATING H20 SYS	1.5970	2.1293	14.3727
.4 STEAM PIPING/VALVES	1.7551	2.3401	15.7960
SUBTOTAL	8.4870	11.3160	76.3832
315 ACCESSORY ELECTRIC	7.4121	6.1767	44.4723
316 MISC. PLANT EQUIP.	0.3683	0.4972	5.4697
317 MHD TOPPING CYCLE			
.1 COMBUSTOR & NOZZLE	0.5609	0.7479	5.0484
.2 MHD GEN & DIFFUSER	1.8611	2.4814	16.7497
.3 MAGNET	4.9127	6.5502	44.2142
.4 INVERTERS	10.3803	13.8404	93.4226
.6 SEED REGENERATION	0.0000	0.0000	0.0000
.7 OXYGEN PLANT	0.0000	0.0000	0.0000
SUBTOTAL	17.7150	23.6200	159.4349
350 TRANSMISSION PLANT	1.4592	1.9456	13.1329
SUBTOTAL	84.6785	94.6809	656.2616
ENGINEERING SERVICES			84.3783
TOTAL ESTIMATED OVERNIGHT CONSTRUCTION COSTS			740.6400
CONSTRUCTION PERIOD -YEARS			5.71
TOTAL ESTIMATED COST INCLUDING INTEREST & ESC DURING CONST IN 1991.5 DOLLARS			817.5288

NOTE: ESCALATION AND INTEREST ARE BASED UPON AN ESTIMATED 6245887. MAN HOURS OF LABOR REQUIRED

Conclusion

Although by today's standards available energy is merely one of the spoils enjoyed by industrialized countries, future standards will be influenced strongly by the growing concern regarding the environment and limited worldwide energy resources. As greater numbers of countries become industrialized, and the world population continues to swell, the demand for clean power will become more and more important to the welfare of the world's inhabitants. To this end, the requirement for efficient and clean power generation needs to be addressed today. The foresight of increasing energy demands can only be met by the development of better energy production techniques.

While few argue about the points above, the development of new technology requires capital funding and this inherently involves bottom line economic considerations. The desire for immediate payoffs is hampering all of the alternative energy research funding efforts. To remain competitive in a free market economy requires the ability to provide goods and/or services for the lowest price possible without sacrificing value. With power grid electricity, the product is the same regardless of the producer so the bottom line involves only the cost of production; though environmental concerns can act as a price offsetting factor. Magnetohydrodynamics fits well with all of the above concerns. The operation of a MHD/steam combined cycle power plant has been studied as a potential high efficiency, low COE, and environmentally friendly electrical energy production method.

The coal-fired MHD generator operation was tested experimentally for years and resulted in an experimental data base but failed to produce the economic benefits promised in theory. The main problems existing today with coal fired MHD operation, namely slag polarization, material durability, and seed regeneration techniques, require further study yet are no longer being funded due to the projected length of time before cost benefits would be available. The movement from coal fuel to natural gas for MHD analysis is one method which may attract future funding since two of the main problems, the slag polarization and seed regeneration, would be clearly affected.

Natural gas fired MHD has been studied in Russia for many years but has not been heavily researched in the United States. The environmental aspects hopefully will change that trend. The MHD generator operates most effectively with sub-stoichiometric conditions which are ideal for the control and minimization of nitrogen oxides. Another environmental benefit involves the reduction of total fuels consumed due to the greater operating efficiency. The magnetohydrodynamic generator has great potential for future energy systems and should be seen as a viable concept in today's energy conscious society. The economic viability for a natural gas MHD/steam combined cycle power plant does exist, as presented above, and when the environmental factor is applied, the reason for further study becomes most apparent.

Recommendations

While the economic analysis provides an optimistic outlook into the operation of a natural gas fired MHD/steam combined cycle power plant, many of the components used in the analysis also require further analysis and advanced development. Specifically a high pressure, high temperature combustor air preheater needs to be developed. Further study into the materials which could be used to build a high temperature combustion air heat exchanger would also be beneficial to other technological areas as well and should also be pursued. The development of the high temperature superconducting materials which could be used in superconducting magnets needs to be continued and methods of reducing costs found. The inherent environmental benefits should be emphasized to gain public support while the low cost of electricity aspects should be put before the utility companies. The time for action regarding improvements to energy policies and promotions of more efficient power plants is right now.

BIBLIOGRAPHY

BIBLIOGRAPHY

Brecha, H., Superconducting Magnet Systems. Heidelberg, Germany: Gebr. Parcus KG, München, 1973.

Burghardt, M. D., and J. A. Harbach, Engineering Thermodynamics, Fourth Edition. New York: HarperCollins, 1993.

Chapman, J. N. "On the Economic Optimization of the Magnetohydrodynamic-Steam Power Plant." Ph.D. Dissertation. The University of Tennessee, Knoxville, 1977.

____________. "Performance Calculations for Mature Technology MHD Steam Combined Cycle Power Plants." University of Tennessee Space Institute, DOE Contract No. DE-AC02-79ET10815, 1979.

____________. et al. "User's Manual for the UTSI MHD/Steam Power Plant Systems Code." University of Tennessee Space Institute, Report No. DOE/ET/10815-98, January 1985.

Choo, Y. K. and P. J. Staiger. "New Features and Applications of PRESTO, A Computer Code for the Performance of Regenerative, Superheated Steam Turbine Cycles." NASA Lewis Research Center. NASA TP-1954. January 1982.

Frost, L. S. "Conductivity of Seeded Atmospheric Pressure Plasmas." Journal of Applied Physics, 32.10 (1961):2029-2036

Fuller, L. C. and T. K. Stoval. "User's Manual for PRESTO: A Computer Code for the Performance of Regenerative Superheated Steam-Turbine Cycles." Oak Ridge National Laboratory. Report No. ORNL-5547, NASA CR-159540. June 1979.

Gordon, S. and B. J. McBride. "Computer Program for the Calculation of Complex Chemical Equilibrium Composition, Rocket Performance and Incident and Reflected Shocks, and Chapman-Jouguet Detonations." NASA Lewis Research Center. NASA SP-273, 1971.

Halliday, D. and R. Resnick. Fundamentals of Physics, Third Edition. New York: John Wiley and Sons, 1974.

Hals, F. A. "Parametric Study of Potential Early Commercial MHD Power Plants Task III--Parameter Variation of Plant Size". NASA Lewis Research Center: Report No. DOE/NASA/0051-3, NASA CR-165445. September 1981.

Handy-Whitman Index of Public Utility Construction Costs. Baltimore , MD: Whitman Requardt and Associates, 1993.

International Energy Annual: 1990. Energy Information Administration. Report No. DOE/EIA-0219(90), January 1992.

Krenz, J. H. Energy: Conversion and Utilization. Boston, MA: Allyn and Bacon, Inc., 1976.

McRae, A. and J. L. Dudas. The Energy Source Book. Germantown, MD: The Center for Compliance Information: an Aspen Publication, 1977.

Munson, B. R., D. F. Young, and T. H. Okiishi. Fundamentals of Fluid Mechanics. New York: John Wiley and Sons, 1990.

Petrick, M. and B. YA. Shumyatsky. Open-Cycle Magnetohydrodynamic Electrical Power Generation. Argonne, Illinois: Argonne National Laboratory, 1978.

Rosa, R. J., Magnetohydrodynamic Energy Conversion. New York: McGraw-Hill Book Company, 1968.

Sawhill, J. C. et al. World Energy Production and Productivity: Proceedings of the International Energy Symposium I. Cambridge, MA: Ballinger Publishing Company, October 1980.

Seikel, G. R. and L. P. Harris. "A Summary of the ECAS MHD Power Plant Results." NASA: Lewis Research Center. Report No. NASA TM X-73491, 1976.

Staiger, P. J. and P. F. Penko. "Summary and Evaluation of the Conceptual Design Study of a Potential Early Commercial MHD Power Plant (CSPEC)." NASA Lewis Research Center. Report No. DOE/NASA/10769-21, NASA TM-82734, January 1982.

Womack, G. J. MHD Power Generation: Engineering Aspects. Great Britain: Willmer Brothers Limited, 1969.

Wu, Y. C. L. "Investigation of the Diagonal Conducting Wall Generator." Proceedings of the 13th Symposium on Engineering Aspects of MHD. Stanford, CA: Stanford University Press, March 1973.

VITA

Daniel Steven Erb was born on June 9, 1964 in Inglewood, California. He is the fourth of six children raised by his parents Robert and Janice. He graduated from Claremont High School, in Claremont, California, in June, 1982. Following a semester at a local junior college, Daniel enlisted in the U. S. Coast Guard on March 19, 1984. While in the Coast Guard he served in Brookings, Oregon as a motor lifeboat crewman for two years, in Sitka, Alaska as a helicopter rescue crewman for another two years, and in Mobile, Alabama as a line maintenance petty officer for his extended term of one year. Daniel was honorably discharged from the Coast Guard on August 18, 1989 after earning a good conduct medal and attaining the position of Aviation Electronics Technician 2nd Class.

Following some prompting from his brother Darrin, he returned to Claremont, California to attend California State Polytechnic University (Cal Poly), Pomona in September, 1989. While attending Cal Poly, Daniel played football as a middle linebacker for three seasons, during each of which he held the position of team captain. At the same time as his youngest sister Michelle received her Marketing degree, he received his Bachelor degree in Mechanical Engineering in June, 1992 (cum laude) and began his graduate study at the University of Tennessee Space Institute in August, 1993 after accepting a graduate research assistant position. Daniel graduated from the Space Institute in December, 1994 where he also served as Student Government President.